

Early myeloid lineage choice is not induced by random PU.1 / GATA1 protein ratios

Philipp S. Hoppe^{1,2}, Michael Schwarzfischer³, Dirk Loeffler^{1,2}, Konstantinos D. Kokkaliaris^{1,2},
Oliver Hilsenbeck^{1,2,3}, Nadine Moritz¹, Max Endeke^{1,2}, Adam Filipczyk¹, Adriana Gambardella⁸,
Nouraiz Ahmed², Martin Etzrodt², Daniel L. Coutu², Michael A. Rieger^{1,4}, Carsten Marr³,
Michael Strasser³, Bernhard Schauburger¹, Ingo Burtscher⁵, Olga Ermakova^{6,8}, Antje Bürger⁷,
Heiko Lickert⁵, Claus Nerlov^{8,9}, Fabian J. Theis^{3,10} and Timm Schroeder^{1,2}

¹ Research Unit Stem Cell Dynamics, ³ Institute of Computational Biology, ⁵ Institute of Diabetes
and Regeneration Research, ⁷ Institute of Developmental Genetics,
Helmholtz Center Munich - German Research Center for Environmental Health (GmbH), 85764
Neuherberg, Germany

² Department of Biosystems Science and Engineering, ETH Zurich, 4058 Basel, Switzerland

⁴ LOEWE Center for Cell and Gene Therapy and Department of Hematology/Oncology, Goethe
University Hospital Frankfurt, 60590 Frankfurt, Germany

⁶ Istituto di Biologia Cellulare e Neurobiologia, CNR, 00015 Monterotondo, Italy

⁸ EMBL Mouse Biology Unit, 00015 Monterotondo, Italy

⁹ MRC Molecular Haematology Unit, Weatherall Institute of Molecular Medicine, University of
Oxford, Oxford OX3 9DS, United Kingdom

¹⁰ Department of Mathematics, Technical University Munich, 85748 Garching, Germany

The mechanisms underlying hematopoietic lineage decisions remain disputed. Lineage-affiliated transcription factors (TFs)^{1,2} with the capacity for lineage reprogramming³, positive auto-regulation^{4,5} and mutual inhibition^{6,7} have been described to be expressed in uncommitted cell populations⁸. This has led to the assumption that lineage choice is cell-intrinsically initiated and made by stochastic switches of randomly fluctuating cross-antagonistic TFs³. However, this hypothesis was developed based on RNA expression data from snapshot and/or population average analyses⁹⁻¹². Alternative models of lineage choice can therefore not be excluded. Here, we use novel reporter mouse lines and live imaging for continuous single cell long-term quantification of PU.1 and GATA1 TF protein levels. We analyse individual hematopoietic stem cells (HSCs) throughout their differentiation into megakaryocytic/erythroid (MegE) and granulocytic/monocytic (GM) lineages. The observed expression dynamics are incompatible with the assumption that stochastic switching between PU.1 and GATA1 precedes and initiates GM versus MegE lineage decision making. Rather, they suggest their involvement only in executing and locking down lineage choice once made. The current prevailing model on early myeloid lineage choice will thus have to be revised.

Multipotent hematopoietic stem and progenitor cells (HSPCs) are thought to differentiate into all blood cell types through a series of progenitor cell types with increasingly restricted lineage potential - like the common myeloid progenitor (CMP), which then further differentiates into GM progenitors (GMPs) or MegE progenitors (MEPs)¹³. The molecular mechanisms controlling lineage choice remain controversial. A prevailing model assumes lineage choice to be initiated and made by stochastic fluctuations of cross-antagonistic TF pairs^{3,14}. It was developed around the hematopoietic TFs PU.1 and GATA1. These are expressed in GM and MegE cells¹³, are required for the production of mature cells of these lineages^{1,2} and can reprogram lineage choice towards their lineages upon overexpression³, respectively. PU.1 and GATA1 proteins can cross-inhibit each other's activity^{6,7} and activate their own transcription^{4,5}. This wiring can generate bi-stable switches, with random higher expression of one TF leading to ever increasing

own expression and repression of competing TFs. PU.1 and GATA1 mRNAs were described to be co-expressed before HSPC lineage choice⁸. Lineage decisions may thus be initiated by random fluctuations of TF levels, breaking a cell's TF equilibrium. The specific wiring of the TF network would lead to specific probabilities for individual TFs to 'win', and thus to stable frequencies of lineage choices. In this model, TFs would not only execute and lock-down, but also initiate and make lineage decisions¹⁴.

However, this model was developed based on expression data of too low resolution to exclude alternative models. Most studies only analysed HSPC population averages⁹⁻¹¹, thus masking cellular heterogeneity^{12,15}, and killed cells to non-quantitatively measure mRNA expression, thus ignoring relevant protein expression dynamics and future lineage choice^{12,16}. We therefore developed approaches for continuous long-term single cell quantification of PU.1 and GATA1 *protein* expression in individual HSPCs from before until after their lineage choice. We created knock-in mouse lines with reading frames for yellow (eYFP) and red (mCHERRY) fluorescent proteins (FPs) knocked into the gene loci for *PU.1* and *Gata1*, respectively (Fig. 1a, Suppl. Fig. 1). The FPs are fused to the TF proteins' C-termini, allowing TF protein quantification by fluorescence intensity. The resulting PU.1eYFP¹⁷ and GATA1mCHERRY mice were mated to create PU.1eYFPxGATA1mCHERRY mice. These are homozygous for both PU.1eYFP and GATA1mCHERRY alleles, males are hemizygous for X-chromosomal GATA1mCHERRY.

As described previously, no² or reduced¹⁸ PU.1 expression or altered PU.1 function¹⁹, and no¹ or altered GATA1 expression²⁰ have drastic phenotypes. In contrast, PU.1eYFPxGATA1mCHERRY mice show no aberrant phenotypes, are born at normal Mendelian ratios (Suppl. Table 1), and did not show increased mortality throughout adulthood (data not shown). The cellular composition of GATA1mCHERRY fetal livers (Suppl. Fig. 2), and adult PU.1eYFPxGATA1mCHERRY peripheral blood and bone marrow (BM) was

unchanged (Fig. 1b-g). Colony-formation *in vitro* was unaltered for PU.1eYFPxGATA1mCHERRY cells (Fig. 1h, i). We could also not observe a difference in GM to MegE lineage output of PU.1eYFPxGATA1mCHERRY versus wild type HSPCs in competitive repopulation assays (Fig. 1j, k; Suppl. Fig. 3). Finally, reprogramming of cells to MegE or GM lineages by GATA1mCHERRY or PU.1eYFP, respectively, was as efficient as with wild type TFs, both in wild type, and in PU.1eYFPxGATA1mCHERRY cells (Suppl. Figs. 4, 5). In conclusion, PU.1eYFP and the GATA1mCHERRY fusion proteins have normal function.

We showed normal expression and stability of the TF-FP fusion proteins by quantitative immunofluorescence staining against PU.1 and GATA1. Simultaneous staining against the TFs and the FPs (Fig. 1l-o) showed high expression correlation and co-localization in HSPC nuclei. Distributions of PU.1 or GATA1 protein expression were not changed in PU.1eYFPxGATA1mCHERRY HSPC populations (Suppl. Figs. 6 and 7), and resembled those read out by fluorescence of the TF-FPs (see below, Fig. 2a). FP fusions to PU.1 and GATA1 therefore did not alter their expression. In addition, we could not detect changes in the stability of PU.1eYFP and GATA1mCHERRY by quantitative immunostaining (Fig. 1p-q) or Western blotting (Suppl. Fig. 8). Thus, although only surrogate reporters, TF-FP fusions can be used²¹ to quantify expression of PU.1 and GATA1 proteins in living HSPCs.

As expected, MEPs highly express GATA1mCHERRY, but only low levels of PU.1eYFP. GMPs express high levels of PU.1eYFP while most are negative for GATA1mCHERRY (Fig. 2a, c). These expression patterns are identical to those previously described for endogenous TFs^{13,22}, and similar, but not the same as for other reporters²³. GATA1 is known to play a role downstream of GMPs²⁴, and a small GMP subpopulation co-expressed PU.1 and GATA1 (Fig. 2a). These cells do not have CMP (GEMMeg) lineage potential, and their strong GM bias suggests that GATA1 does not play a role in these cells' GM versus MegE lineage decision (data

not shown). PU.1^{mid}GATA1^{mid} progenitors mostly had only MegE potential (Fig. 2b). PU.1⁻GATA1^{high} cells are more mature and have lost colony potential (Fig2b).

HSPCs are described to express both PU.1 and GATA1 mRNA before MegE versus GM lineage choice^{8,10,11}. We therefore expected CD34⁺CD16/32⁻c-Kit⁺Sca-1⁻lineage⁻ CMPs¹³ to co-express both TFs. However, their vast majority express either only high PU.1 levels, or GATA1 with low or no PU.1 expression. These are already committed to the GM and MegE lineage, respectively (Fig. 2d). Thus, this ‘CMP’ population is in fact a mixture of already committed GMPs and MEPs²². HSCs already express intermediate levels of PU.1eYFP, but no GATA1mCHERRY (Fig. 2a). To identify the expected HSPC population with GEMMeg potential downstream of PU.1^{mid}GATA1⁻ HSCs and upstream of already committed CMPs/GMPs/MEPs, we analysed the whole lineage⁻ Sca-1⁻c-Kit⁺ (LSK) progenitor population (Fig. 2a). As in another GATA1 reporter mouse²³ only few LSK cells expressed GATA1mCHERRY. The earliest HSPC population in which we could detect a small but robust GATA1mCHERRY⁺ expressing subpopulation was the MPP2 population^{25,26} (Fig. 2e). However, this GATA1⁺ MPP2 subpopulation is already MegE committed (see below).

The PU.1/GATA1 switch model is based on near-stoichiometric PU.1 and GATA1 co-expression, and thus mutual functional inhibition, before GM versus MegE lineage decision^{6,7}. In contrast, we could not identify a PU.1eYFP⁺GATA1mCHERRY⁺ HSPC population with robust GEMMeg potential. However, this data from snapshot FACS analysis cannot exclude that differentiating PU.1^{mid}GATA1⁻ HSCs may quickly pass through a state with similar PU.1 and GATA1 expression. We therefore extended approaches for long-term imaging and single cell tracking^{27,28,21} to allow continuous live quantification of PU.1eYFP and GATA1mCHERRY in differentiating HSPCs. Detection of PU.1eYFP and GATA1mCHERRY fluorescence was better by imaging than by FACS, with higher sensitivity and greater dynamic range (Fig. 3a-e). TF protein numbers in individual cells were estimated by comparison to defined amounts of

recombinant FPs in Western blot analyses (Fig. 3f, g and Suppl. Table 2). HSCs were cultured under conditions allowing both MegE and GM differentiation, which were detected by expression of GATA1mCHERRY or CD16/32¹³, respectively (Fig. 4a-e, Suppl. Fig. 9). While these culture conditions do not resemble all possible *in vivo* conditions, they do allow differentiation into all relevant lineages, thus enabling to analyse the core mechanisms underlying MegE versus GM lineage choice.

We quantified absolute PU.1 and GATA1 protein levels in single differentiating HSCs and their progeny, over up to 11 generations (Fig. 4f, Suppl. Fig. 10). About 6.5×10^6 total, including 3.7×10^5 (1.8×10^5 manually curated) fluorescence, measurements in four experiments with 1080 CD16/32 and 681 GATA1mCHERRY onsets from 256 different HSC colonies were analysed (Suppl. Table 3).

As expected, cells differentiating into the GM-lineage increased their PU.1eYFP levels over time and later expressed CD16/32 (Fig. 4g, first and second panel, Suppl. Movie 1). Unexpectedly, we never detected GATA1mCHERRY expression at any point during GM differentiation. This is in contrast to the expectations from the prevailing model of the PU.1/GATA1 switch as the initiator of this lineage choice. Our detection limit for GATA1mCHERRY is about 1900 molecules per cell. In about half of all GM differentiations, PU.1eYFP levels steadily increased from the starting HSC until the onset of CD16/32 expression. In the other half, PU.1eYFP levels transiently dropped, before then steadily increasing. However, only $25 \pm 5\%$ of all GM time courses showed PU.1 numbers dropping below 8100 molecules (the average expression in HSCs). Moreover, only about $1\% \pm 1\%$ of GM differentiating cells transiently dropped to below 2000 PU.1 molecules, and thus to similar levels of potentially maximally expressed GATA1 molecules. GATA1 levels thus do not play a relevant role during GM differentiation.

Whenever cells expressed detectable GATA1mCHERRY, during HSC differentiation or in freshly sorted GATA1⁺ MPP2s, they always further differentiated into PU.1eYFP⁺

GATA1mCHERRY⁺ MegE cells (Fig. 4g, third and fourth panel, Suppl. Video 2). This confirms GATA1 expression onset as a marker for MegE lineage commitment (Fig. 4c-e, Supp. Fig. 9). Importantly, this was independent of PU.1 levels during GATA1 expression onset, demonstrating that PU.1/GATA1 ratios do not regulate MegE commitment. In addition, PU.1eYFP levels already decreased before detectable GATA1mCHERRY expression in $63 \pm 19\%$ of cases (compare Fig. 4g, third panel). GATA1 expression thus is not the cause of PU.1 down-regulation. In all remaining cases, GATA1 was upregulated while PU.1 was still expressed at different levels. However, in these cases, cells later always differentiated into a PU.1⁻ GATA1^{high} MegE state, demonstrating that different PU.1 levels during lineage decision making are irrelevant for the start of GATA1 expression.

In conclusion, we did not observe any reproducible PU.1/GATA1 double positive stage through which all differentiating HSCs pass (Fig. 4h). PU.1 and GATA1 are independently regulated at the start of GM versus MegE differentiation. These observed protein dynamics are incompatible with random and cross-regulatory PU.1/GATA1 co-expression to be the central mechanism to initiate MegE versus GM lineage choice³. This conclusion is in line with observations that lineage choice is still possible after deletion of PU.1 or GATA1, where only further maturation of committed cells is impaired^{1,2,29}. Our data is compatible with that from other reporter mice²³. However, it also demonstrates discrepancies between protein and mRNA expression in uncommitted HSPCs^{8,30} - the latter of which had originally led to the development of currently prevailing models.

While we demonstrate that ratios of total PU.1/GATA1 protein numbers are not the central mechanism in initiating HSPC lineage decisions, we cannot exclude that only a very small subset of expressed PU.1 proteins may be active to compete with potentially existing GATA1 protein expressed below our detection limit. The PU.1/GATA1 switch may be involved in the lineage choice of other cell types²⁴ not analysed here. Likewise, other TF switches could be involved in

GM versus MegE or other lineage choices. We conclude that physical PU.1/GATA1 interaction and antagonism^{6,7} could serve as an execution and/or lock-down mechanism making terminal differentiation irreversible, but not as a decision making mechanism inducing it. We expect other TFs and signalling pathways activated by extracellular signals to be upstream regulators of lineage specific TFs. Their complex interplay will be of interest for future analyses.

References

1. Pevny, L. *et al.* Erythroid differentiation in chimaeric mice blocked by a targeted mutation in the gene for transcription factor GATA-1. *Nature* **349**, 257–60 (1991).
2. Scott, E. W., Simon, M. C., Anastasi, J. & Singh, H. Requirement of transcription factor PU.1 in the development of multiple hematopoietic lineages. *Science* **265**, 1573–7 (1994).
3. Graf, T. & Enver, T. Forcing cells to change lineages. *Nature* **462**, 587–94 (2009).
4. Tsai, S. F., Strauss, E. & Orkin, S. H. Functional analysis and in vivo footprinting implicate the erythroid transcription factor GATA-1 as a positive regulator of its own promoter. *Genes Dev.* **5**, 919–31 (1991).
5. Chen, H. *et al.* PU.1 (Spi-1) autoregulates its expression in myeloid cells. *Oncogene* **11**, 1549–60 (1995).
6. Zhang, P. *et al.* PU.1 inhibits GATA-1 function and erythroid differentiation by blocking GATA-1 DNA binding. *Blood* **96**, 2641–8 (2000).
7. Nerlov, C., Querfurth, E., Kulesa, H. & Graf, T. GATA-1 interacts with the myeloid PU.1 transcription factor and represses PU.1-dependent transcription. *Blood* **95**, 2543–51 (2000).
8. Miyamoto, T. *et al.* Myeloid or lymphoid promiscuity as a critical step in hematopoietic lineage commitment. *Dev. Cell* **3**, 137–47 (2002).
9. Huang, S., Guo, Y.-P., May, G. & Enver, T. Bifurcation dynamics in lineage-commitment in bipotent progenitor cells. *Dev. Biol.* **305**, 695–713 (2007).
10. Akashi, K. *et al.* Transcriptional accessibility for genes of multiple tissues and hematopoietic lineages is hierarchically controlled during early hematopoiesis. *Blood* **101**, 383–9 (2003).
11. Månsson, R. *et al.* Molecular evidence for hierarchical transcriptional lineage priming in fetal and adult stem cells and multipotent progenitors. *Immunity* **26**, 407–19 (2007).
12. Hoppe, P. S., Coutu, D. L. & Schroeder, T. Single-cell technologies sharpen up mammalian stem cell research. *Nat. Cell Biol.* (2014). doi:10.1038/ncb3042
13. Akashi, K., Traver, D., Miyamoto, T. & Weissman, I. L. A clonogenic common myeloid progenitor that gives rise to all myeloid lineages. *Nature* **404**, 193–7 (2000).

14. Orkin, S. H. & Zon, L. I. Hematopoiesis: an evolving paradigm for stem cell biology. *Cell* **132**, 631–44 (2008).
15. Etzrodt, M., Ende, M. & Schroeder, T. Quantitative single-cell approaches to stem cell research. *Cell Stem Cell* **15**, 546–58 (2014).
16. Kueh, H. Y., Champhekar, A., Nutt, S. L., Elowitz, M. B. & Rothenberg, E. V. Positive feedback between PU.1 and the cell cycle controls myeloid differentiation. *Science* **341**, 670–3 (2013).
17. Kirstetter, P., Anderson, K., Porse, B. T., Jacobsen, S. E. W. & Nerlov, C. Activation of the canonical Wnt pathway leads to loss of hematopoietic stem cell repopulation and multilineage differentiation block. *Nat. Immunol.* **7**, 1048–56 (2006).
18. Rosenbauer, F. *et al.* Acute myeloid leukemia induced by graded reduction of a lineage-specific transcription factor, PU.1. *Nat. Genet.* **36**, 624–30 (2004).
19. Moreau-Gachelin, F. *et al.* Spi-1/PU.1 transgenic mice develop multistep erythroleukemias. *Mol. Cell. Biol.* **16**, 2453–63 (1996).
20. Heyworth, C., Pearson, S., May, G. & Enver, T. Transcription factor-mediated lineage switching reveals plasticity in primary committed progenitor cells. *EMBO J.* **21**, 3770–81 (2002).
21. Filipczyk A, Marr C, Schwarzfischer M, Feigelmann J, Hastreiter S, Hoppe PS, Loeffler D, Kokkaliaris KD, Ende M, Schauburger B, Hilsenbeck O, Hasenauer J, Anastasiadis K, Theis FJ, S. T. Network Plasticity of Pluripotency Transcription Factors in Embryonic Stem Cells. *Nat. Cell Biol.* (2015).
22. Pronk, C. J. H. *et al.* Elucidation of the phenotypic, functional, and molecular topography of a myeloerythroid progenitor cell hierarchy. *Cell Stem Cell* **1**, 428–42 (2007).
23. Arinobu, Y. *et al.* Reciprocal activation of GATA-1 and PU.1 marks initial specification of hematopoietic stem cells into myeloerythroid and myelolymphoid lineages. *Cell Stem Cell* **1**, 416–27 (2007).
24. Iwasaki, H. *et al.* Identification of eosinophil lineage-committed progenitors in the murine bone marrow. *J. Exp. Med.* **201**, 1891–7 (2005).
25. Miyawaki, K. *et al.* CD41 marks the initial myelo-erythroid lineage specification in adult mouse hematopoiesis: redefinition of murine common myeloid progenitor. *Stem Cells* **33**, 976–87 (2015).

26. Pietras, E. M. *et al.* Functionally Distinct Subsets of Lineage-Biased Multipotent Progenitors Control Blood Production in Normal and Regenerative Conditions. *Cell Stem Cell* (2015). doi:10.1016/j.stem.2015.05.003
27. Rieger, M. A., Hoppe, P. S., Smejkal, B. M., Eitelhuber, A. C. & Schroeder, T. Hematopoietic cytokines can instruct lineage choice. *Science* (80-.). **325**, 217–8 (2009).
28. Eilken, H. M., Nishikawa, S.-I. & Schroeder, T. Continuous single-cell imaging of blood generation from haemogenic endothelium. *Nature* **457**, 896–900 (2009).
29. Mancini, E. *et al.* FOG-1 and GATA-1 act sequentially to specify definitive megakaryocytic and erythroid progenitors. *EMBO J.* **31**, 351–65 (2012).
30. Hu, M. *et al.* Multilineage gene expression precedes commitment in the hemopoietic system. *Genes Dev.* **11**, 774–85 (1997).
31. Liu, P., Jenkins, N. A. & Copeland, N. G. A highly efficient recombineering-based method for generating conditional knockout mutations. *Genome Res.* **13**, 476–84 (2003).
32. Shaner, N. C. *et al.* Improved monomeric red, orange and yellow fluorescent proteins derived from *Discosoma* sp. red fluorescent protein. *Nat. Biotechnol.* **22**, 1567–72 (2004).
33. Dymecki, S. M. Flp recombinase promotes site-specific DNA recombination in embryonic stem cells and transgenic mice. *Proc. Natl. Acad. Sci. U. S. A.* **93**, 6191–6 (1996).
34. Kiel, M. J. *et al.* SLAM family receptors distinguish hematopoietic stem and progenitor cells and reveal endothelial niches for stem cells. *Cell* **121**, 1109–21 (2005).
35. Wilson, A. *et al.* Hematopoietic Stem Cells Reversibly Switch from Dormancy to Self-Renewal during Homeostasis and Repair. *Cell* **135**, 1118–1129 (2008).
36. Schwarzfischer, M. *et al.* in *Proc. Microsc. Image Anal. with Appl. Biol.* (2011).
37. Kreutz, C. *et al.* An error model for protein quantification. *Bioinformatics* **23**, 2747–53 (2007).

Methods

Generation of *Gata1*mCHERRY knock-in mice

The knock-in construct was cloned by using conventional restriction enzyme mediated cloning and recombineering³¹ using the BAC RPCIB731C02198Q (Source BioScience) that contained the *Gata1* locus. The final knock-in construct consisted of a 5.0 kbp 5'-homology arm lasting until the last codon of *Gata1* (skipping the endogenous stop-codon) followed by a short linker sequence (AGAGCATCAGGTACCAGTGGAGCT), the coding sequence for mCHERRY³² and a FRT-flanked phospho-glycerate kinase (PGK) promoter-driven neomycin (neo) resistance gene and the 4.6 kbp 3'-homology arm. After removal of the neo selection marker, the GATA1mCHERRY fusion mRNA transcript utilizes the endogenous 3'UTR.

JM8 mouse ES cell lines derived from the C57BL/6N strain were grown on gelatinized tissue culture plates. Cells were maintained in Knockout DMEM (Gibco) supplemented with 2 mM glutamine, 1% β -mercaptoethanol (360 μ l in 500 ml PBS, sterile-filtrated), 10–15% fetal calf serum (Invitrogen) and 500 U ml⁻¹ ESGRO leukemia-inhibitory factor (Millipore).

Electroporations of ES cells were carried out in a 25-well cuvette using the ECM 630 96-well electroporator / HT-200 automatic plate handler (BTX Harvard Apparatus; set at 700 V, 400 Ω , 25 μ F). Immediately before electroporation, cell suspensions of $\sim 10^7$ cells and ~ 2.5 μ g of linearized targeting vector DNA were mixed in a final volume of 120 μ l PBS. Cells were seeded onto a gelatinized 10-cm dish and colonies were picked after 8-9 d of puromycin (3 μ g/ml) selection. The colonies were expanded in 4 copies of 96-well plates for archiving and characterization. Cells were frozen in supplemented Knockout DMEM with 10% DMSO and stored in vapor over liquid nitrogen. After identification of positive clones, cells were thawed and expanded for aggregation.

Correctly targeted ES cell clones were identified by Southern blot using probes at the designated locations (Suppl. Fig. 1) after digestion of genomic DNA with the restriction enzymes BamHI and XbaI, respectively. PCR primers for generating the Southern probes from BAC DNA were CAGCCACTGCCCAAATAGGTGGAG and CTCCACCTATTTGGGCAGTGGCTG (5'-

probe) and CTGAAGTGGTGCTCTGGACTTTAC and TGAGGAAGAGGGAAGGATGTGAAG (3'-probe).

From one ES cell clone, germline chimeras were generated by ES cell aggregation with CD1 morulae and the FRT-flanked neo selection cassette was deleted *in vivo* by a Flp-e deleter strain by recombinase-mediated excision³³.

Genotyping

PCR Primers for checking presence/absence of the NEO cassette were GCATGGACGAGCTGTACAAG, CTGCACGAGACTAGTGAGAC and GCAGGAGAATGGGAAATGTG leading to a 223 bp band after successful removal. Unsuccessful removal would have led to a 387 bp band. Primers for checking the presence/absence of Flp-recombinase were GTTCTATATGCTGCCACTCC and GAGCGATAAGCGTGCTTCTG leading to 176 bp band at its presence. GATA1(mCHERRY) mice were genotyped using the primers GCATGGACGAGCTGTACAAG, AGGTACTGCCCCACCTCTATC and GCAGGAGAATGGGAAATGTG leading to a 297 bp band in the case of wt *Gata1* and a 223 bp band in the case of *Gata1mCHERRY*.

Isolation and staining of primary HSPCs and blood

Mice for blood counts, bone marrow analysis, and time-lapse movies were sacrificed at the age of 12-16 weeks. Blood counts were quantified on an Abc Animal Blood Counter (scil animal care company). The following parameters were quantified (Fig. 1b): wbc = white blood cells ($200/\text{mm}^3$), rbc = red blood cells ($4 \cdot 10^5/\text{mm}^3$), plt = platelets ($4 \cdot 10^2/\text{mm}^3$), hgb = haemoglobin (0.4 g/dl), hct = haematocrit (%), mcv = mean corpuscular volume (μm^3), mch = mean corpuscular haemoglobin (0.4 pg), mchc = mean corpuscular haemoglobin concentration (g/dl), rdw = red cell distribution width (0.4 %), mpv = mean platelet volume ($0.2 \mu\text{m}^3$), lypro = % lymphocytes of wbc (2 %), mopro = % monocytes of wbc (0.1 %), grpro = % granulocytes of wbc (%), eopro = % eosinophils of wbc (0.2 %). Isolation of primary cells and FACS sorting was performed as described^{13,22,34,35}. All flow cytometry was performed on a FACS Aria I or III (BD Bioscience). In brief, pelves, femurs, tibiae, humeri and vertebrae of adult mice were isolated, crushed and incubated with anti-CD16/32 antibody (clone 2.4G2, BD Pharmingen, or clone 93, eBioscience) prior to staining with the desired antibody cocktail. If cells were prepared

for sorting HSCs, they were subjected to ACK Lysing Buffer (Lonza) after crushing followed by a lineage depletion using biotinylated CD3e (clone 145-2C11), CD11b (clone M1/70), CD19 (clone 1D3), CD41 (clone MWReg30), B220 (clone RA3-6B2), Gr-1 (clone RB6-8C5) and TER-119 (clone TER-119, all eBioscience) antibodies and Streptavidin-conjugated beads Roti-MagBeads (Carl Roth). The following antibodies were further used for staining: anti-CD34 (RAM34), anti-CD48 (HM48-1), anti-CD105 (MJ7/18), anti-CD117 (2B8), anti-CD117 (ACK2), anti-CD135 (A2F10), anti-Sca-1 (D7, all eBioscience) and anti-CD150 (TC15-12F12.2, BioLegend). Different HSPC types within the Lineage⁻Sca-1⁺c-Kit⁺ (LSK) population (Fig. 1c) were identified as: HSC = LSK CD150⁺CD34⁻CD48⁻, MPP1 = LSK CD150⁺CD34⁺CD48⁻, MPP2 = CD150⁺CD34⁺CD48⁺, MPP3/4 = CD150⁻CD34⁺CD48⁺. When cells were prepared for sorting myeloid progenitors, CD41-Biotin was omitted. CD41 was also omitted for the analysis of the MPP subpopulations (Fig. 2e). Single-cell sorts into 384-well plates (Greiner Bio-One) were performed according to manufacturer's instructions on a FACSARIAIII (BD Bioscience). E14.5 fetal livers were isolated, individualized, and stained with antibodies for analysis. For GATA1 protein numbers quantification, GATA1mCHERRY⁺ cells were sorted. For GATA1mCHERRY Cycloheximide experiments, cells from bulk fetal livers from C57BL/6 and GATA1mCHERRY knock-in mice at a ratio of 1:1 were used.

Colony assays

All colony assays were performed in Methocult GF M3434 (STEMCELL Technologies) according to manufacturer's instructions.

Competitive transplantations

After ACK lysis (Life Technologies), freshly isolated bone marrow from CD45.1 homozygous C57BL/6 wt mice was mixed 1:1 with bone marrow from either CD45.2 homozygous C57BL/6 wt mice or CD45.2 homozygous PU.1eYFPxGATA1mCHERRY mice. Cells were frozen in 90% IMDM (Life Technologies) / 10% DMSO (Sigma Aldrich) and stored above liquid nitrogen until further usage. For transplantations, cells were thawed, counted and 10⁶ living cells were transplanted into the tail vein of lethally irradiated CD45.1/CD45.2 heterozygous mice. Lineage contribution of donor cell mixtures was determined by bone marrow harvest and staining²² after 6-7 weeks.

Immunostainings

Immunostainings were performed after permeabilization with 0.2% Triton-X (Applichem) with 8 µg/ml anti-PU.1 (T-21), 8 µg/ml anti-GATA1 (N6) (both Santa Cruz), 10 µg/ml anti-GFP (Aves Labs) and 5 µg/ml anti-mCHERRY (ab167453) (Abcam) primary antibodies in 10% donkey serum in TBS-T (Tris-buffered saline, 0.1% Tween 20) over night at 4 °C, three washing steps of each 5 minutes and 10 µg/ml AlexaFluor dyes conjugated donkey secondary antibodies (Jackson ImmunoResearch) for 1 h at room temperature in 10% donkey serum in TBS-T. Images were acquired on a Nikon Eclipse Ti-E microscope. Fluorescent signals were quantified by segmentation of nuclear DAPI staining and background subtraction (without 'gain') as described³⁶.

Cycloheximide treatment and Western blot analysis

In order to compare transcription factors and their fusions regarding their biochemical behaviour cells were kept in medium additionally supplied with 50 µM Cycloheximide and split into several vials. For immunostainings, cells were transferred to poly-L-lysine (Sigma Aldrich) coated object slides, stored for 10 minutes at 4 °C, fixed with paraformaldehyde (Sigma-Aldrich), stored at 4 °C and stained (see above). For Western blotting, cells were spun down at designated time points and directly lysed in Laemmli-buffer, boiled at 100 °C and frozen at -20 °C until further usage in SDS-Polyacrylamide electrophoresis. In the case of protein number quantification, designated amounts of recombinant GFP (Clontech) and mCHERRY (ChromoTek) were used. Gels were run on a 10% SDS-gel, blotted onto a PVDF-membrane (BioRad) and incubated with one of the following antibodies: anti-GATA1 (N6) (Santa Cruz), anti-PU.1 (9G7) (Cell Signaling), anti-GFP (7.1, 13.1) (Roche), anti-mCHERRY (1C51) (abcam). Chemiluminescence was detected using horseradish peroxidase conjugated secondary antibodies (Jackson), ECL Plus Western Blotting Detection Reagents (GE Healthcare) and medical x-ray films (Fujifilm). Signal intensities were quantified using ImageJ software.

Cytospins

Cells were spun on object slides following manufacturer's instructions (Hettich), dried, and stained with May-Gruenwald (Carl Roth) and Giemsa solution (Sigma-Aldrich).

Time-lapse image acquisition and tracking

Time-lapse imaging was performed at 37 °C in fibronectin (Takara Bio) coated channel slides μ -slide VI^{0,4} (ibidi), in StemSpan SFEM (STEMCELL Technologies) medium supplemented with 100 ng/ml SCF, 100 ng/ml TPO, 10 ng/ml IL-3, 10 ng/ml IL-6 (all PeproTech), 5 U/ml EPO (PromoKine), 50 U/ml Penicillin, 50 μ g/ml Streptomycin (Invitrogen), self-labelled Alexa Fluor 647 (Invitrogen) anti-CD16/32 antibody (2.4G2) and 5% CO₂ using an Axio Observer Z1 microscope (Zeiss). A HXP 120 (Zeiss) was used as fluorescent light source. 46HE, 43HE (both Zeiss) and Cy5 (AHF) filter sets were used to detect eYFP, mCHERRY and Alexa Fluor® 647, respectively, at exposure times between 400-1500 ms. Brightfield pictures were acquired every 60-120 seconds, fluorescent pictures for the quantification of PU.1eYFP and GATA1mCHERRY were acquired every 30 minutes and every 3-4 hours for the detection of CD16/32-Alexa Fluor® 647. Pictures that were used for quantifications were saved in lossless TIF or PNG format. Single-cell tracking and image quantification were performed by self-written software as described^{27,28}.

Inference of absolute protein numbers

Western blot dilution assays

For protein number quantification, known cell numbers of PU.1eYFP^{high} progenitors and GATA1mCHERRY⁺ E14.5 fetal livers cells were resolved by Western blotting on 10% polyacrylamide gels and compared with different levels of recombinant GFP protein (Clontech) or mCHERRY (antibodies-online.com). PU.1eYFP, GATA1mCHERRY, GFP, and mCHERRY proteins were detected using an anti-GFP primary antibody (Roche) or an anti-mCHERRY antibody (Abcam). All quantifications of band intensities were performed by ImageJ software by manually drawing a gate around the bands and subtracting the mean of the same area above and below the bands for primary HSPCs.

Model

After comparing several models to describe the data, we found a sigmoidal function to best describe the relationship between the dilution of the standard x and the observed intensity y :

$$y(x) = \left(\frac{\lambda x^n}{K^n + x^n} \right) \cdot \epsilon(x) \quad (1)$$

Here, the exponent n determines the steepness of the sigmoidal, K sets the inflection point, λ is the maximum of the curve and ϵ is a lognormally distributed error term with expectation 1 and standard deviation σ as suggested for western blot data³⁷. This model outperformed other models like linear models with and without intercept according to the BIC and coefficient of variation between replicates. We estimate model parameters using 10,000 local optimizations initialized according to Latin-hypercube sampling.

We determine the number of proteins P_j per cell from the sample intensity y_j of replicate j (i.e. western blot) as

$$P_j = \frac{K_j}{\left(\frac{\lambda_j}{y_j} - 1 \right)^{\frac{1}{n_j}}} \cdot \frac{1}{c \cdot w} \quad (2)$$

where c equals number of loaded cells and w is the molecular weight for the protein of interest. The first term is obtained by solving Eq (2) for x , whereas the second term relates dilution in nanogram to absolute protein numbers per cell. The parameters λ_j , K_j , n_j have been obtained by the local optimization.

Error propagation

As P_j is a combination of uncertain variables, we obtained errorbars for each P_j individually by applying standard error propagation to account for uncertainties in the number of cells c (we assume a standard deviation of 10%) and uncertainties in the model (estimated via the standard deviation σ of our noise model ϵ_i in Eq (1)). However, we find that the uncertainties for each individual replicate P_j are always with a factor <0.3 smaller than the inter-replicate standard deviations. Therefore, we only consider the standard deviation across replicates, as this is the dominate source of uncertainty in our procedure.

Mapping protein numbers to different HSPC populations

Inference

From reference cell types used for Western blot dilution assays, we map mean protein numbers to all other cell types using the mean fluorescence intensities from flow cytometry. Since we

observe fluorescence intensities from fusion protein levels, we assume a linear relation between FACS intensities and molecule numbers. We obtain the average protein amount per FACS intensity of our reference cell type r as $\psi_r = \frac{\overline{P^{(r)}}}{\overline{MFI^{(r)}}}$. Here, $\overline{MFI^{(r)}}$ is the mean fluorescence intensity of our protein of interest in the reference population (e.g. PU.1eYFP^{high}) used for the western blotting, averaged over N replicates: $\overline{MFI^{(r)}} = \frac{1}{N} \sum_{i=1}^N MFI_i^{(r)}$. By $\overline{P^{(r)}}$ we denote the estimated amount of protein from western blotting via Eq (2), averaged over three replicates j . We calculate the average amount of protein in any other population of interest (e.g. GMPs) as

$$\overline{P^{(GMP)}} = \psi_r \cdot \overline{MFI^{(GMP)}} = \frac{\overline{MFI^{(GMP)}}}{\overline{MFI^{(r)}}} \cdot \overline{P^{(r)}},$$

where $\overline{MFI^{(GMP)}}$ is the mean fluorescence intensity of our protein of interest in the GMP population averaged over N replicates.

Error Propagation

To obtain errorbars for the protein amount in a population of interest, we perform error propagation, taking into account the uncertainty $\Delta P^{(r)}$ in protein numbers (as describe above, we only consider inter-replicate variation), as well as uncertainty in the mean fluorescence intensities (standard deviation ΔMFI_i over the MFI_i) (e.g. GMPs):

$$\Delta P^{(GMP)} = \sqrt{(\Delta MFI^{(GMP)})^2 \cdot \left(\frac{\overline{P^{(r)}}}{\overline{MFI^{(r)}}}\right)^2 + (\Delta MFI^{(r)})^2 \cdot \left(\frac{\overline{MFI^{(GMP)}} \cdot \overline{P^{(r)}}}{(\overline{MFI^{(r)}})^2}\right)^2 + (\Delta P^{(r)})^2 \cdot \left(\frac{\overline{MFI^{(GMP)}}}{\overline{MFI^{(r)}}}\right)^2}$$

Mapping protein numbers to movie intensity

The mean fluorescence intensity of the first timepoints was used to calibrate PU.1eYFP protein abundance in time-lapse experiments. Whenever a movie cell exceeds twice the detection limit in the GATA1mCHERRY channel for more than 5 consecutive time points, the cell itself and all its descendants were annotated as GATA1mCHERRY positive. Mean protein abundance of GATA1 positive movie cells has been calibrated to the mean protein abundance of PU.1^{mid}GATA1^{mid} in flow cytometry. Protein levels are then interpolated linearly³⁷.

Single-cell tracking and fluorescence quantification

Single-cell tracking was performed as described. Briefly, self-written software allows following individual cell identities over many days in order to generate genealogy trees. Fluorescence image normalization has been applied as described³⁶. Custom written software semi-automatically identifies shapes of tracked cells and quantifies protein levels resulting in normalized intensity time traces independently of timing and location in time-lapse imaging. Detection thresholds were determined by simulating *in silico* background cells based on manually selected pixels containing only background signal and based on manually inspected cell areas. The 99% quantile of the resulting distribution of *in silico* background cells is referred to the detection threshold which is extrapolated to protein numbers for each movie as described above.

Supplementary Information accompanies the paper on www.nature.com/nature.

Acknowledgments We are grateful to S. Ammersdoerfer, H. Oller, C. Raithel, B. Vogel and A. Ziegler for technical support. This work was supported by the ERC (starting grant Latent Causes), the German Federal Ministry of Education and Research (BMBF), the German Research Foundation (DFG) within the SPPs 1395 (InKoMBio) and 1356 to F.J.T., and DFG SFB 684 to T.S and the SNF to T.S.. T.S., S.S. and O.H. acknowledge financial support from SystemsX.ch.

Author Contributions P.S.H. planned and performed experiments and analysed data; M.Sc. programmed and applied quantitative imaging software and performed protein quantification and statistical analysis with M.St., C.M. and F.J.T.. M.Sc., D.L., K.K, M.En., N.M., M.A.R., N.A., M.Et, M.A.R, and A.F. provided support for time-lapse imaging, flow cytometry and software development. O.H. and B.S. programmed single-cell tracking software with T.S.. D.L.C contributed to immunofluorescence staining. I.B., H.L. and A.B. contributed to generation of GATA1mCHERRY mice. O.E, A.G. and C.N. provided the PU.1eYFP mouse and competitive transplantations. F.J.T. designed and supervised the data analysis and modelling part. T.S.

designed the study, programmed software, analysed data and wrote the paper with P.S.H. All authors read and commented on the final manuscript.

Author Information Reprints and permissions information is available at npg.nature.com/reprintsandpermissions. The authors declare no competing financial interests. Correspondence and requests for materials should be addressed to T.S. (timmm.schroeder@bsse.ethz.ch).

Figure Legends

Figure 1: Normal haematopoiesis in PU.1YFPxGATA1mCHERRY double homozygous mice

a: Structure of endogenous gene loci after knock-in. Black boxes: exons. b-g: Normal haematopoiesis in PU.1eYFPxGATA1mCHERRY double homozygous mice. b: Peripheral blood counts of adult mice (n = 6 and 9). See materials for abbreviations. No significant difference, one-way MANOVA ($p > 0.09$). c-g: Composition of adult BM (n = 4). One-way MANOVA for panels c-g: $p = 0.35/0.35/0.03/0.31/0.16$, respectively. h-k: Normal lineage choice of PU.1eYFPxGATA1mCHERRY HSPCs. h,i : Colony-forming assay from whole BM or HSCs (mean + s.d., n = 3 each), respectively. No significant difference for each population (Wilcoxon rank sum test, p-values > 0.2 and > 0.4 , respectively). Meg = megakaryocytic, E = erythroid, M = monocytic, G = granulocytic. j-k: Competitive transplantation of BM donor cells (CD 45.2) with identical numbers of wt competitor cells (CD45.1) into CD45.1/CD45.2 recipients. j, k: PreMegE/PreGM and MegE/GM ratios of donor cells at 6-7 weeks after transplantation (Suppl. Fig. 3); no significant difference (Wilcoxon rank sum test, $p = 0.97$ and $p = 0.84$, respectively). l-o: Immunostaining against PU.1 and eYFP (l-m) or GATA1 and mCHERRY (n-o), day 7 of HSC differentiation. Representative examples from three experiments. DAPI: nuclei, Scale bar = 10 μm . p-q: Normal stability of TF-FP fusions. PU.1(eYFP) or GATA1(mCHERRY) protein decay after 50 μM Cycloheximide treatment of GMPs or PreMegE-cells, respectively. Data from quantitative immunostaining against PU.1 or GATA1.

Figure 2: PU.1eYFP and GATA1mCHERRY expression in HSPCs

a: Flow cytometry analysis of adult BM HSPCs (representative example of 4 experiments). LSK = Lineage⁻Sca-1⁺c-Kit⁺, LK = Lineage⁻Sca-1⁻c-Kit⁺. b: Colony forming assay (mean \pm s.d.) of PU.1eYFP^{high}GATA1mCHERRY⁻ (clonogenicity 39.6% \pm 7.1%, n = 3), PU.1eYFP^{high}GATA1mCHERRY^{mid} (clonogenicity 32.2% \pm 11.4%, n = 4), PU.1eYFP^{mid}GATA1mCHERRY^{mid} (clonogenicity 37.1% \pm 11.9%, n = 4) and PU.1eYFP⁻GATA1mCHERRY^{high} (clonogenicity 0%, n = 3) LK cells, see dashed boxes in (a). Blast = blast colonies. c: Fold-changes of PU.1eYFP fluorescence intensity in flow cytometry (mean \pm s.d., n = 4, one representative example shown). d: Colony forming assay of PU.1eYFP⁺GATA1mCHERRY⁻ and GATA1mCHERRY⁺ CMPs (clonogenicity 58.4% \pm 14.4% and 46.3% \pm 10.4%, respectively), see dashed boxes in (a), mean \pm s.d (n = 3). e: Representative example of GATA1mCHERRY expression in MPP1-4³⁵. GATA1⁺ MPP2s are MegE committed (see text).

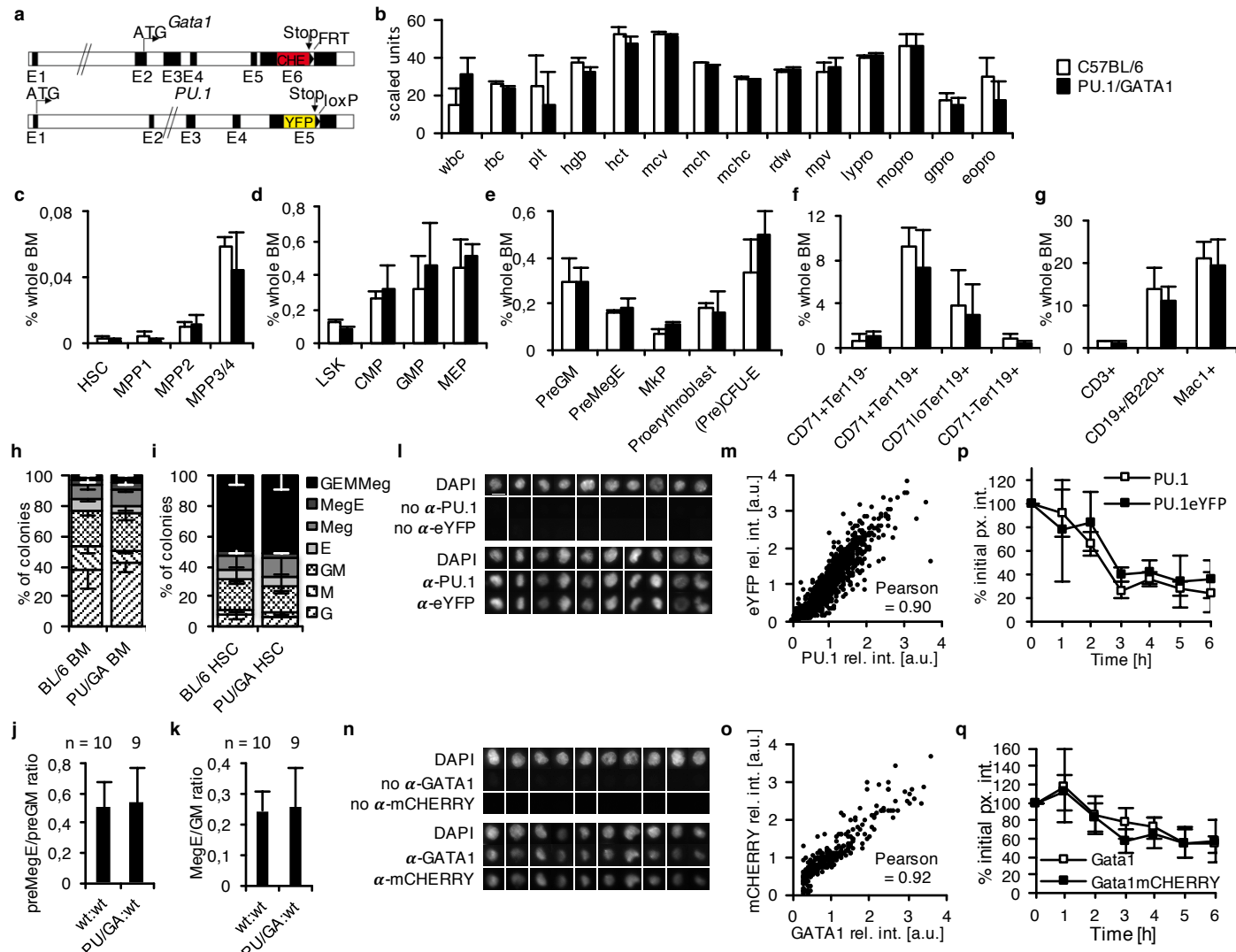
Figure 3: Reliable quantification of PU.1eYFP and GATA1mCHERRY protein numbers by live cell imaging

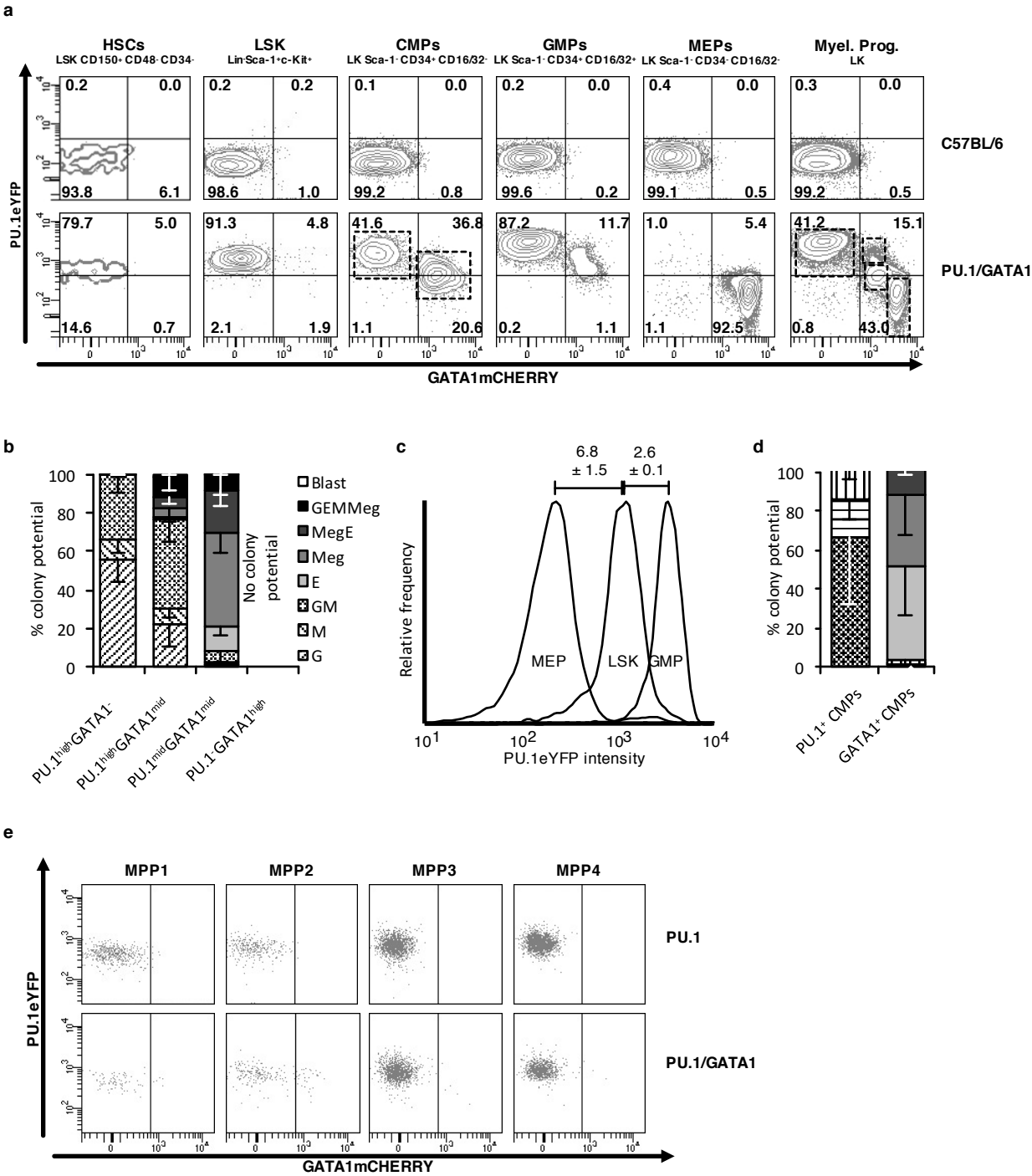
a-b: Different HSPCs were sorted (a) and quantitatively imaged (b). Scale bar: 50 μm . c: Fold-changes aligned to the detection threshold (mean \pm s.d, $n = 4$ for flow cytometry, $n = 3$ for imaging). Representative examples. d-e: Better sensitivity (d, mean percentages \pm s.d. of cells gated as in (a) above detection threshold) and dynamic range (e, mean \pm s.d.) of imaging and flow cytometry. f: Quantification of molecule numbers in sorted PU.1eYFP⁺ BM LK cells and E14.5 GATA1mCHERRY⁺ fetal liver cells by comparison to defined amounts of recombinant eGFP and mCHERRY, respectively. Representative examples, respectively ($n = 3$). * incomplete loading of sample. g: Estimation of molecule numbers in populations designated in (a). Mean protein abundance per cell. Error bars include uncertainty from western blot quantification and fold-changes of flow cytometry or imaging, respectively (mean \pm s.d).

Figure 4: Single cell dynamics refute random PU.1/GATA1 ratios as inducers of early myeloid lineage choice

a: CD16/32 and GATA1mCHERRY expression in differentiating HSCs (flow cytometry). Mean \pm s.d.; n = 3 (day 4), n = 1 (day 5, 6). Colony differentiation dynamics are shown in Supp Fig. 9. b: Colony potential of differentiating HSCs on day 5-7 of culture (mean \pm s.d., n = 3). GM = colony containing CD16/32 expressing cells, Mega = colony containing megakaryocytes, GEMMeg = colony containing GM and Meg, \emptyset = colony containing neither GM nor Meg. c: Flow cytometry sorting scheme of day 4 HSC culture. GATA1mCHERRY and CD16/32 are mutually exclusive. d: Colony potential of sorted cells from (c). Mean \pm s.d (n = 3). e: Cytospin of cells from day 4 cultures. Scale bars: 10 μ m. f: Single-cell genealogy of a differentiating HSC over 6 days. CD16/32 detection by live-antibody staining, megakaryocytes determined by cell morphology. 'X': cell death, '?': lost cell identity. g: Typical traces of PU.1 and GATA1 expression of GM (first and second panel) or MegE differentiating cells (third and fourth panel). h: Time resolved density scatter plot of PU.1eYFP and GATA1mCHERRY expression levels in differentiating HSCs. Data electronically synchronized to the onset (t = 0h) of CD16/32 and GATA1mCHERRY, respectively. Light blue circle highlights initial expression profile of HSCs (see also Suppl. Movie 3).

Figure 1





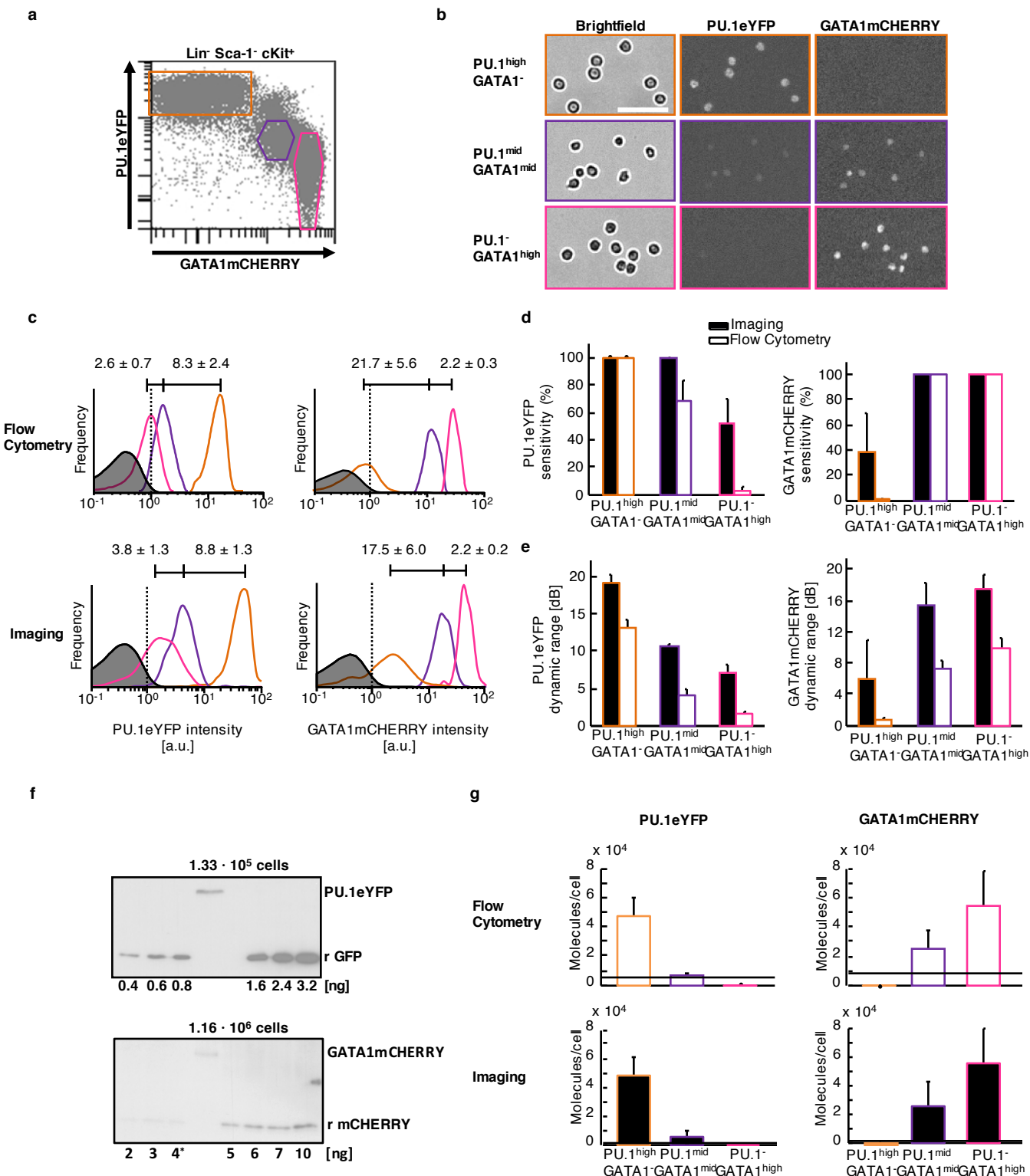
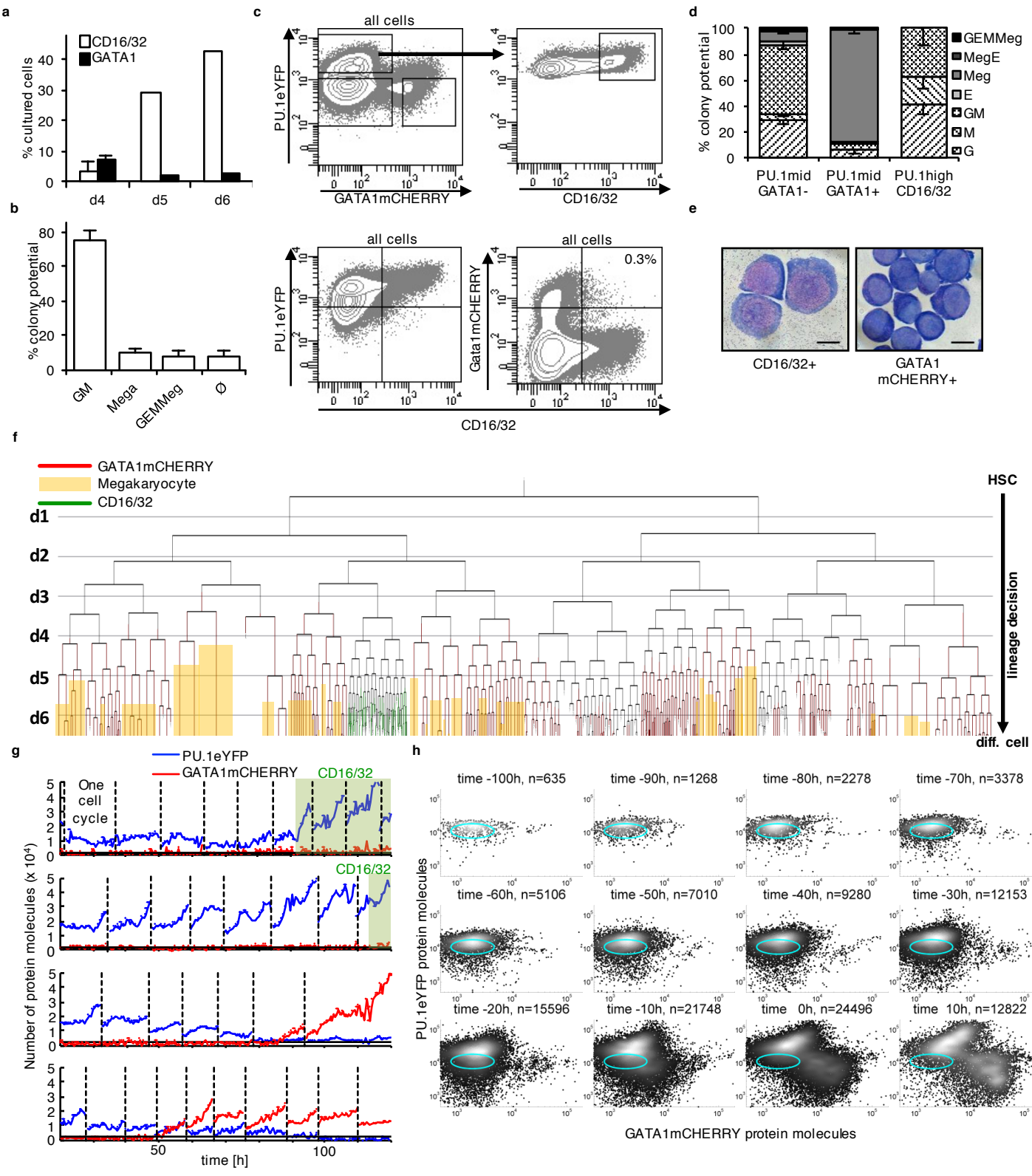
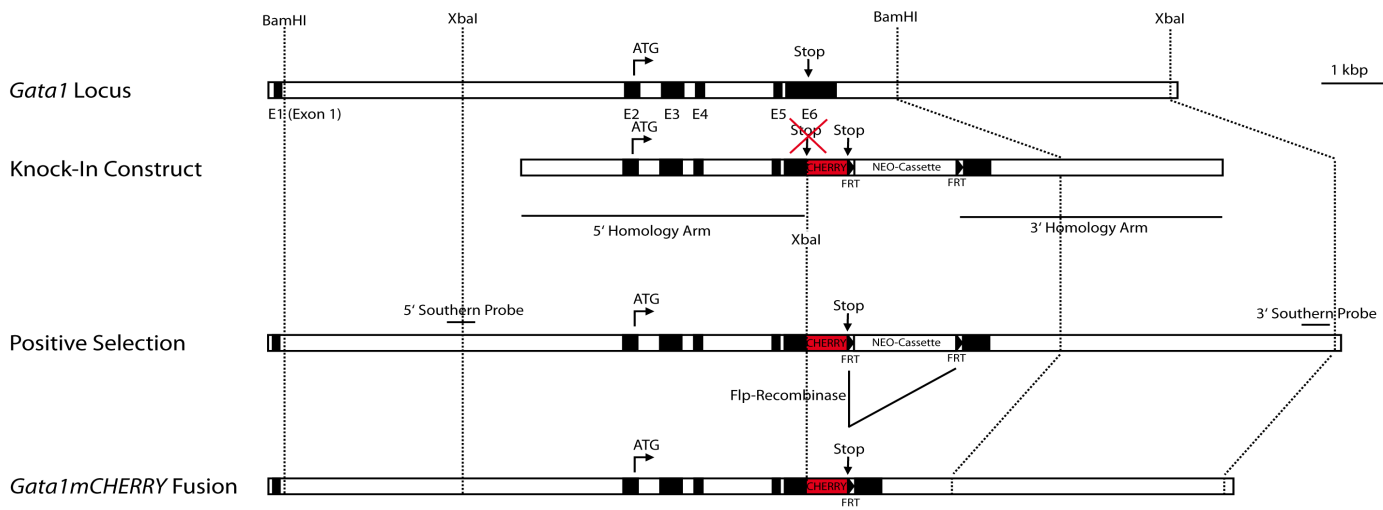


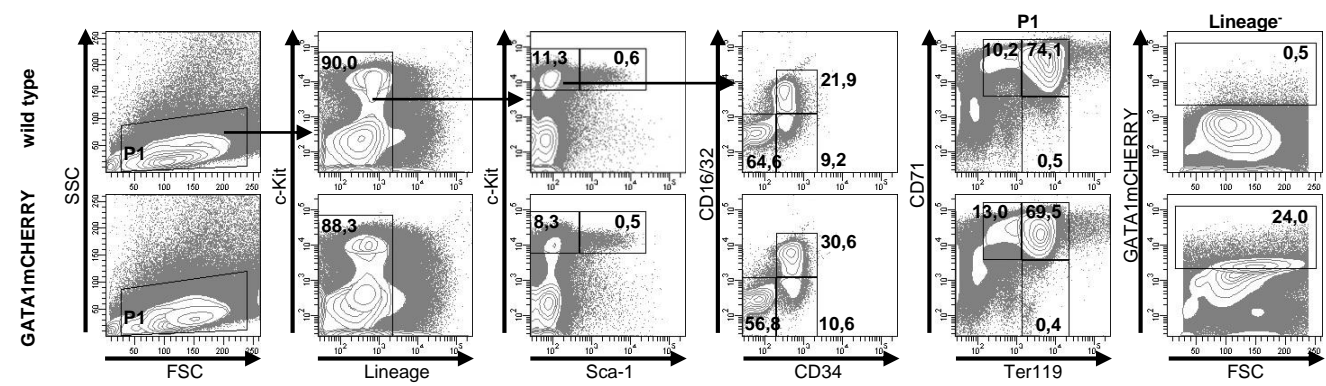
Figure 4





Supplementary Figure 1 | Knock-in strategy for the insertion of *mCHERRY* into the endogenous *Gata1* locus

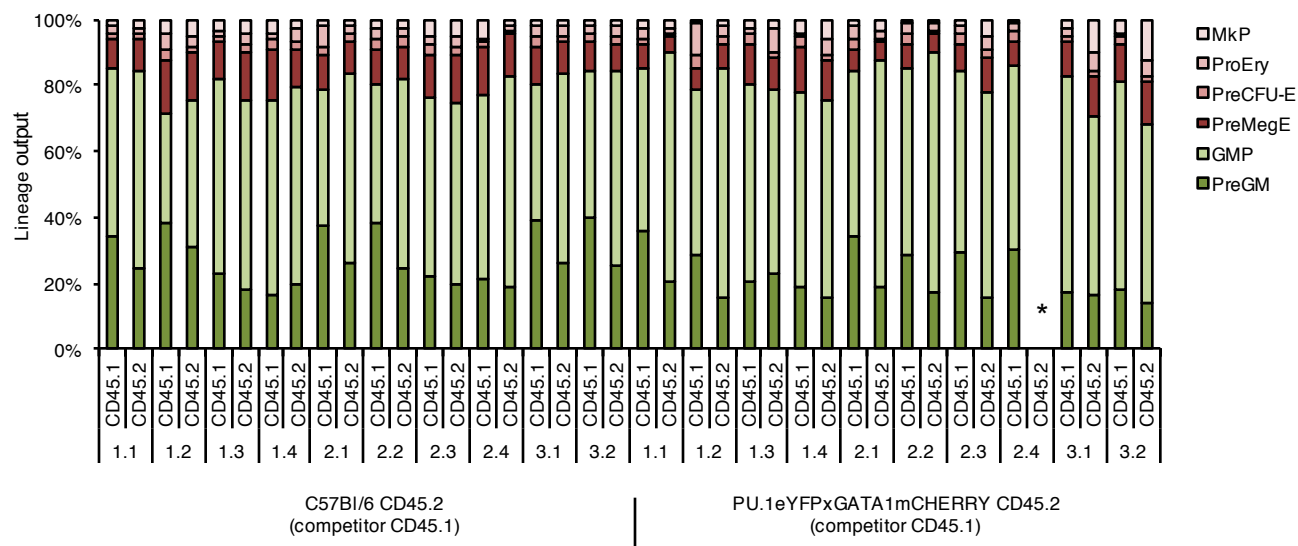
Overview of Gata1mCHERRY knock-in strategy. BamHI and XbaI were chosen as suitable restriction enzymes in order to generate restriction fragment length polymorphisms (from 11.1 kbp to 5.7 kbp in the case of XbaI and from 9.9 kbp to 11.1 kbp in the case of BamHI) for screening successful knock-ins. Genomic sequences for Southern probes were identified at designated locations. The final knock-in construct contained a 5.0 kilo base pairs (kbp) long 5' homology arm lasting until the last codon of Gata1, a short linker sequence (AGAGCATCAGGTACCAGTGGAGCT), the open reading frame (ORF) of mCHERRY, a FRT-flanked Neomycin-resistance cassette (including a eukaryotic and a prokaryotic promoter and a polyadenylation signal) and a 4.6 kbp long 3' homology arm.



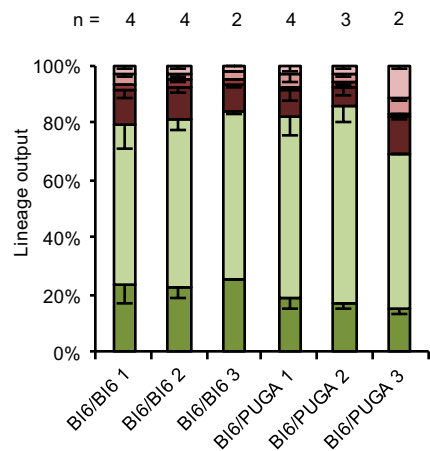
Supplementary Figure 2 | E14.5 fetal livers of GATA1mCHERRY mice have the same composition as C57BL/6 wildtype fetal livers

Fetal livers (FL) of E14.5 embryos were collected, subjected to Ficoll-density centrifugation, pooled (C57BL/6 7 FLs, GATA1mCHERRY 6 FLs) and analysed by flow cytometry. Shown are percentages of the parental gate.

a



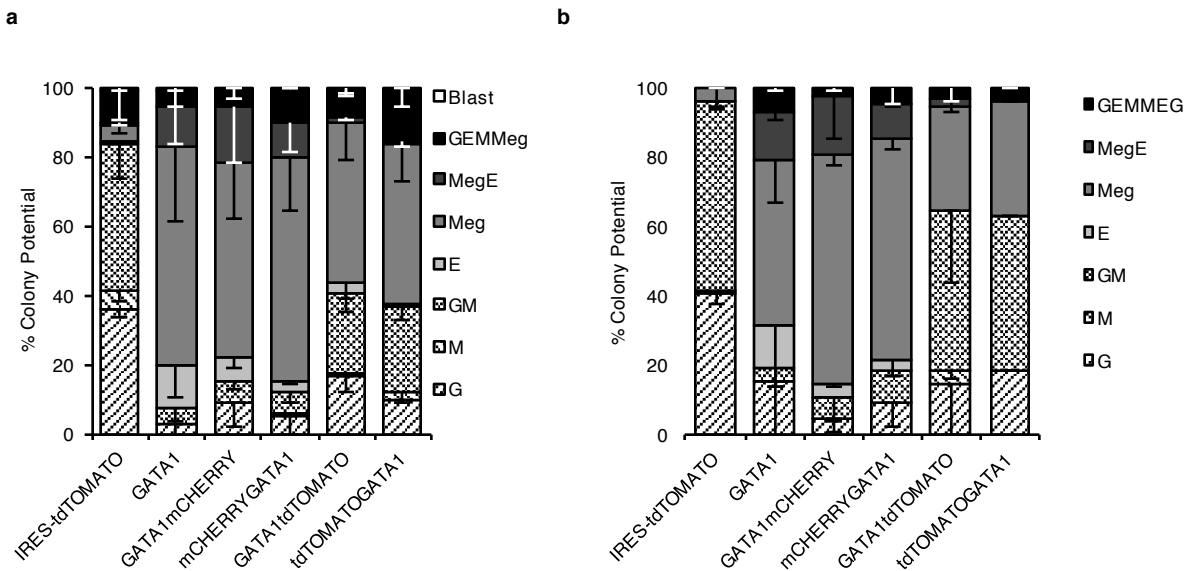
b



Supplementary Figure 3 | MegE vs. GM-lineage contribution *in vivo* is unaltered in cells from GATA1mCHERRY/PU.1eYFP mice upon competitive transplantation

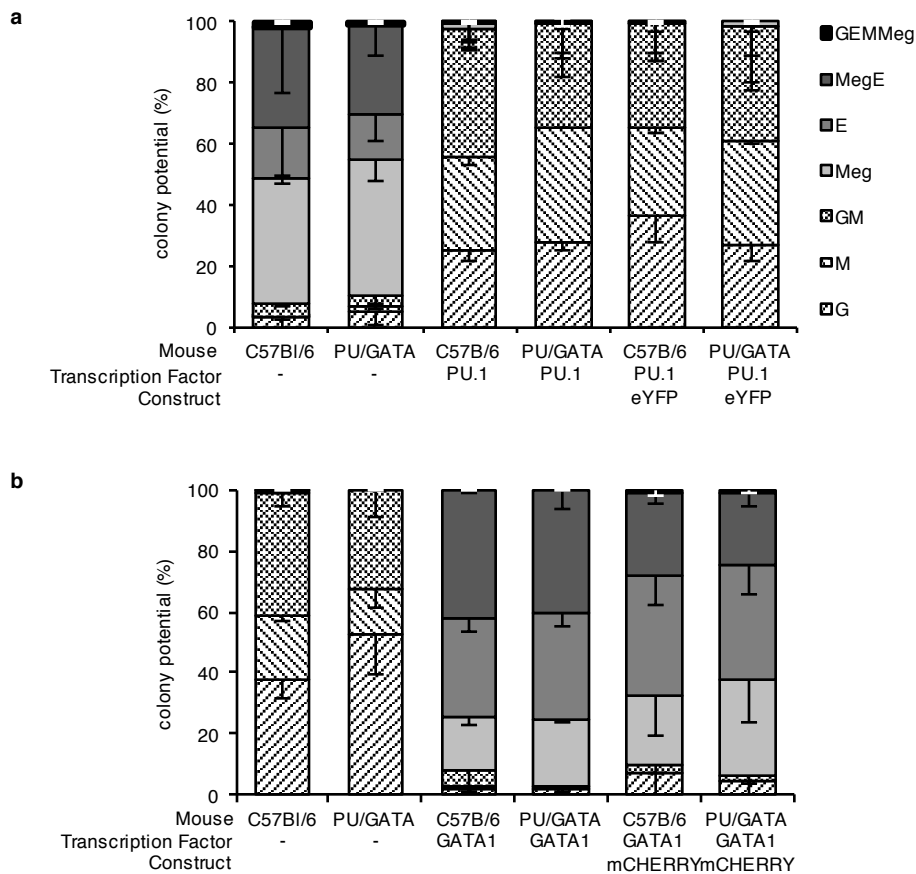
a) 10⁶ bulk bone marrow cells in a 1/1 ratio from CD45.1 C57Bl/6 and CD45.2 C57Bl/6 or from CD45.1 C57Bl/6 and CD45.2 PU.1eYFPxGATA1mCHERRY mice were transplanted into lethally irradiated recipient mice and bone marrow progenitor cell composition was analysed after 7-8 weeks. X.Y numbers denote donor pair (X) and recipient mouse (Y). MkP=megakaryocyte progenitor, ProEry=proerythroblast, PreCFU-E=pre colony-forming unit erythrocyte, PreMegE=pre megakaryocyte erythrocyte progenitor , PreGM=pre granulocyte macrophage progenitor. * data excluded due to low contribution.

b) Summarized bone marrow lineage contribution per donor pair (a).



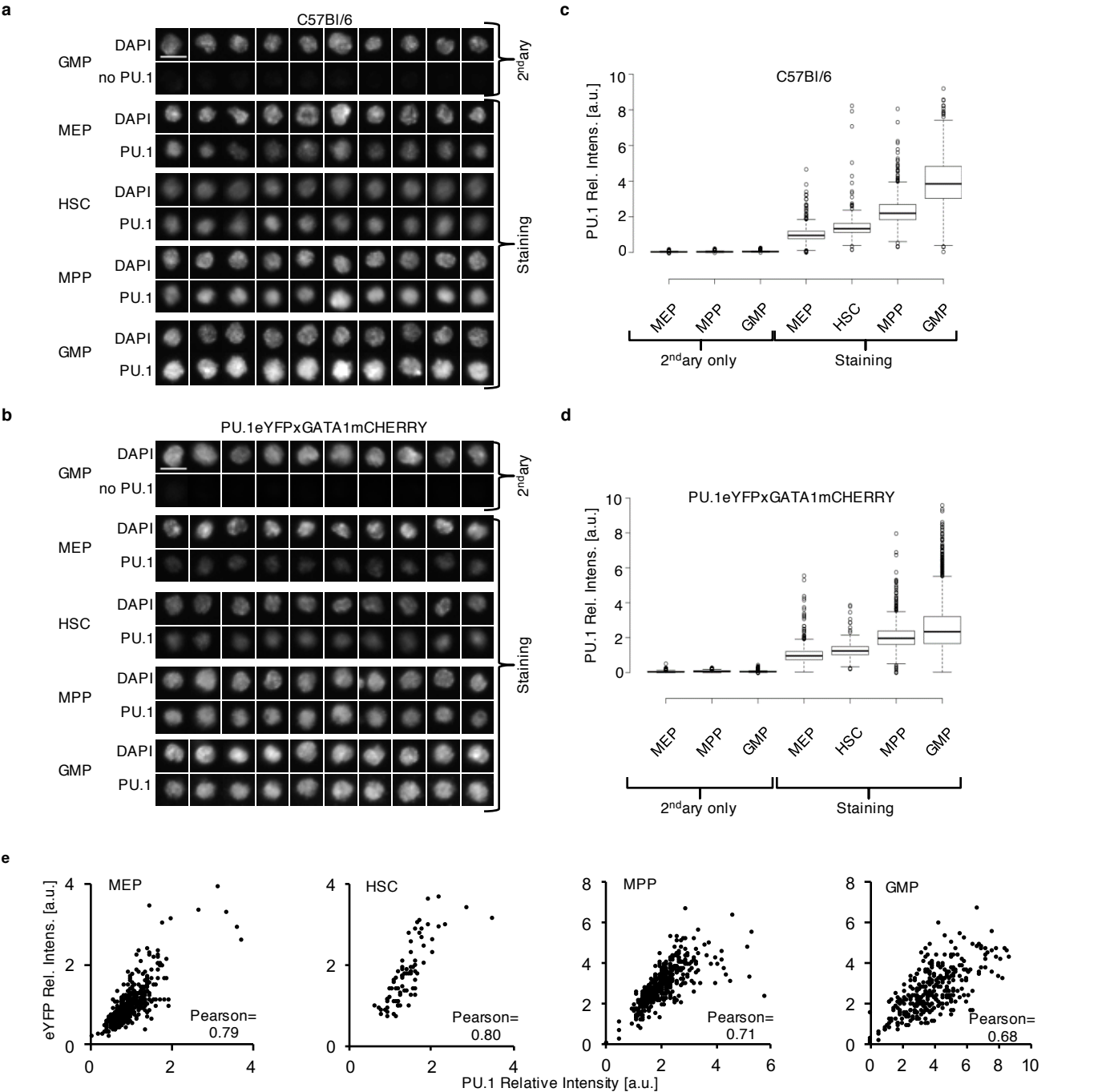
Supplementary Figure 4 | Fusions of GATA1 with mCHERRY reprogram as efficiently as GATA1 wildtype protein

a-b, LSK CD34⁺ Flt3⁺ were sorted, infected with lentivirus expressing the designated proteins and plated in methylcellulose under permissive conditions. Cells from C57BL/6 mice (**a**) (n = 3) and cells from PU.1eYFP knock-in mouse (n = 2, except tdTOMATOGATA1 n = 1) (**b**) were used. Data are mean ± s.d.. GEMMeg = granulocytic/erythroid/monocytic/megakaryocytic, MegE = megakaryocytic/erythroid, Meg = megakaryocytic, E = erythroid, GM = granulocytic/monocytic, M = monocytic, G = granulocytic



Supplementary Figure 5 | Reprogramming capacity of PU.1eYFP and GATA1mCHERRY is unaltered compared to their wild-type counterparts in both wild-type and PU.1eYFPxGATA1mCHERRY cells

PreMegE cells (a) or PreGM cells (b) from both C57Bl/6 wild-type and PU.1eYFP/GATA1mCHERRY (,PU/GATA^{-/-}) knock-in mice were sorted and transduced with mock (,-), PU.1 or PU.1eYFP expressing lentivirus (a) or with mock (,-), GATA1 or GATA1mCHERRY expressing lentivirus (b), respectively. After 24 hours, cells were seeded in methylcellulose under permissive conditions. Colonies were scored after 8-10 days of culture (n = 3-4). A Kruskal-Wallis test did not detect any significant difference between groups C57Bl/6 PU.1, PU/GATA PU.1, C57Bl/6 PU.1eYFP and PU/GATA PU.1eYFP for each cell population independently (p-value > 0.77). By including groups C57Bl/6 and PU/GATA significant differences (for M, Meg and E, p-value < 0.05) are observed. A Kruskal-Wallis test did not detect any significant difference between groups C57Bl/6 GATA1, PU/GATA GATA1, C57Bl/6 GATA1mCHERRY and PU/GATA GATA1mCHERRY for each cell population independently (p-value > 0.23). By including groups C57Bl/6 and PU/GATA a significant difference (for MegE, p-value < 0.007) is observed. Data are mean ± s.d.. GEMMeg = granulocytic/erythroid/monocytic/megakaryocytic, MegE = megakaryocytic/erythroid, Meg = megakaryocytic, E = erythroid, GM = granulocytic/monocytic, M = monocytic, G = granulocytic

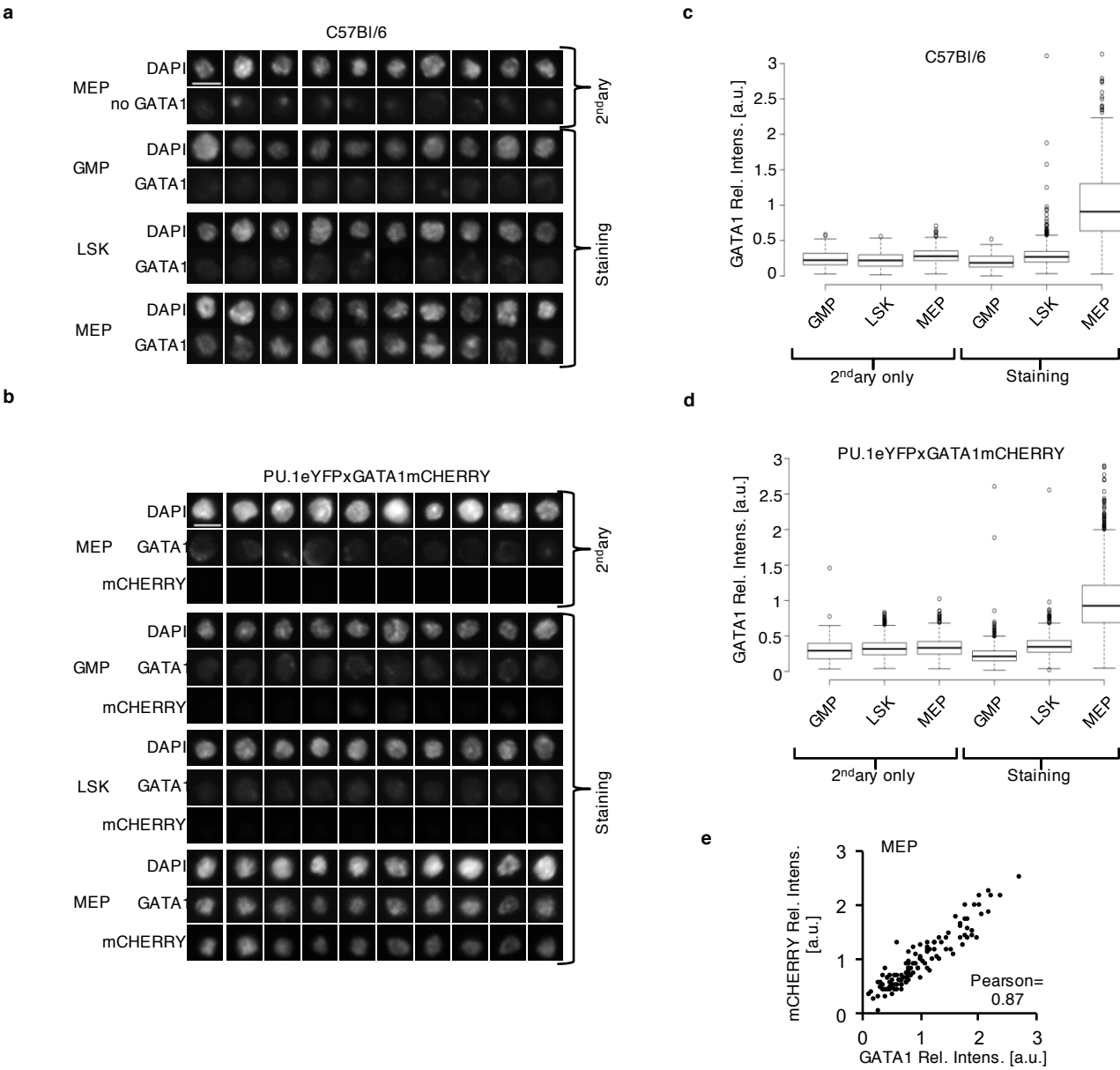


Supplementary Figure 6 | PU.1 is expressed in nuclei of all HSCs, MPPs, GMPs and MEPs of wildtype and GATA1mCHERRY/PU.1eYFP mice and overlaps with eYFP expression.

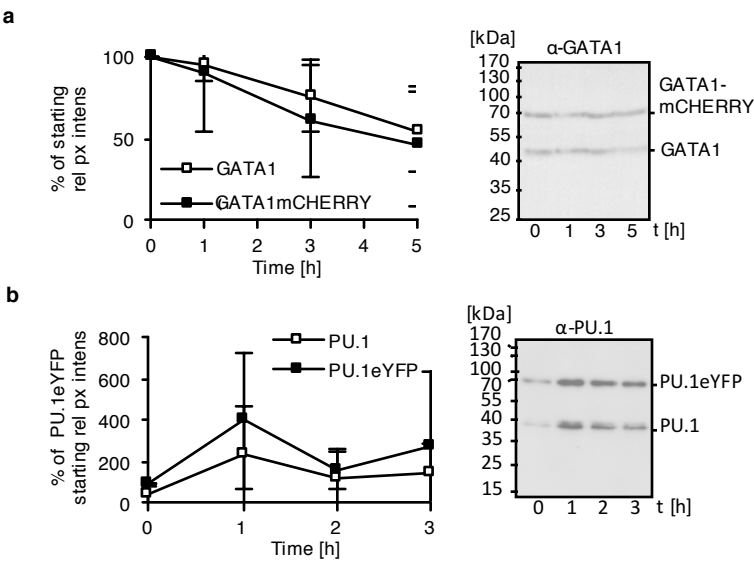
a-b) Indicated cell populations from wildtype C57Bl/6 (a) and PU.1eYFPxGATA1mCHERRY (b) mice were sorted, fixed and probed with PU.1 antibody followed by staining with secondary antibody. Representative examples from controls ("2ndary", without primary antibody) and stainings of GMPs, MPPs, HSCs and MEPs (CD150⁺ progenitors) are shown. DAPI allowed the staining of nuclei. Scale bar = 10 μ m.

c-d) Quantifications of relative PU.1 expression levels determined by pixel intensities. Data includes samples from 3 independent experiments, each of which was normalized to the mean expression levels of the respective MEP population. Individual data points for (c) are 884 MEP 2ndary only (475, 148 and 261 data points from the individual experiments), 1218 MPP 2ndary only (553, 260 and 405), 755 GMP 2ndary only (599, 122 and 34), 1213 MEP (659, 371 and 183), 603 HSCs (360, 194 and 49), 1458 MPP (749, 283 and 426) and 819 GMP (571, 183 and 65). Individual data for (d) points are 1530 MEP 2ndary only (739, 449 and 342 data points from the individual experiments), 1194 MPP 2ndary only (547, 394 and 253), 1866 GMP 2ndary only (1616, 126 and 124), 1521 MEP (518, 581 and 422), 273 HSCs (116, 79 and 78), 1531 MPP (616, 463 and 452) and 2339 GMP (1351, 673 and 315).

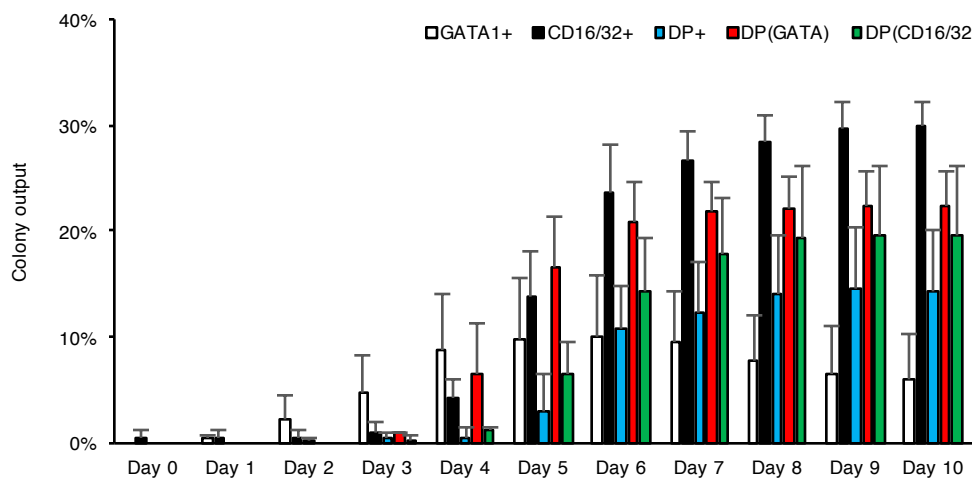
e) Correlation plot of PU.1 and eYFP staining in the indicated cell populations from one experiment. Pixel intensities were normalized to the mean expression in MEPs. Pearson correlation coefficient is displayed. Mean Pearson correlation values of all three experiments were 0.82 ± 0.04 (MEP), 0.69 ± 0.10 (HSC), 0.71 ± 0.06 (MPP) and 0.63 ± 0.08 (GMP), respectively.



Supplementary Figure 7 | GATA1 is only expressed in nuclei of MEPs of wildtype and PU.1eYFPxGATA1mCHERRY mice and overlaps with mCHERRY expression.
a-b) Indicated cell populations from wildtype C57Bl/6 (a) and PU.1eYFPxGATA1mCHERRY (b) mice were sorted, fixed and probed with GATA1 (a,b) and mCHERRY (b) antibody followed by staining with secondary antibodies. Representative examples from controls (“2ndary”, without primary antibody) and stainings of GMP, LSK and MEP (CD150⁺ progenitors) are shown. DAPI allowed the staining of nuclei. Scale bar = 10 μ m.
c-d) Quantifications of relative GATA1 expression levels determined by pixel intensities. Data includes samples from 3 independent experiments, each of which was normalized to the mean expression levels of the respective MEP population. Individual data points for (c) are 292 GMP 2ndary only (56, 188 and 48 data points from the individual experiments), 698 LSK 2ndary only (155, 287 and 256), 563 MEP 2ndary only (308, 216 and 39), 344 GMP (64, 158 and 122), 1167 LSK (394, 294 and 479) and 590 MEP (252, 155 and 183). Individual data points for (d) are 485 GMP 2ndary only (171, 173 and 141 data points from the individual experiments), 1295 LSK 2ndary only (360, 552 and 383), 886 MEP 2ndary only (561, 203 and 122), 462 GMP (73, 114 and 275), 1184 LSK (252, 441 and 491) and 865 MEP (632, 115 and 118).
e) Correlation plot of GATA1 and mCHERRY staining in the indicated cell populations from one experiment. Pixel intensities were normalized to the mean expression in MEPs. Pearson correlation coefficient is displayed. Mean Pearson correlation values of all three experiments was 0.87 ± 0.06 .

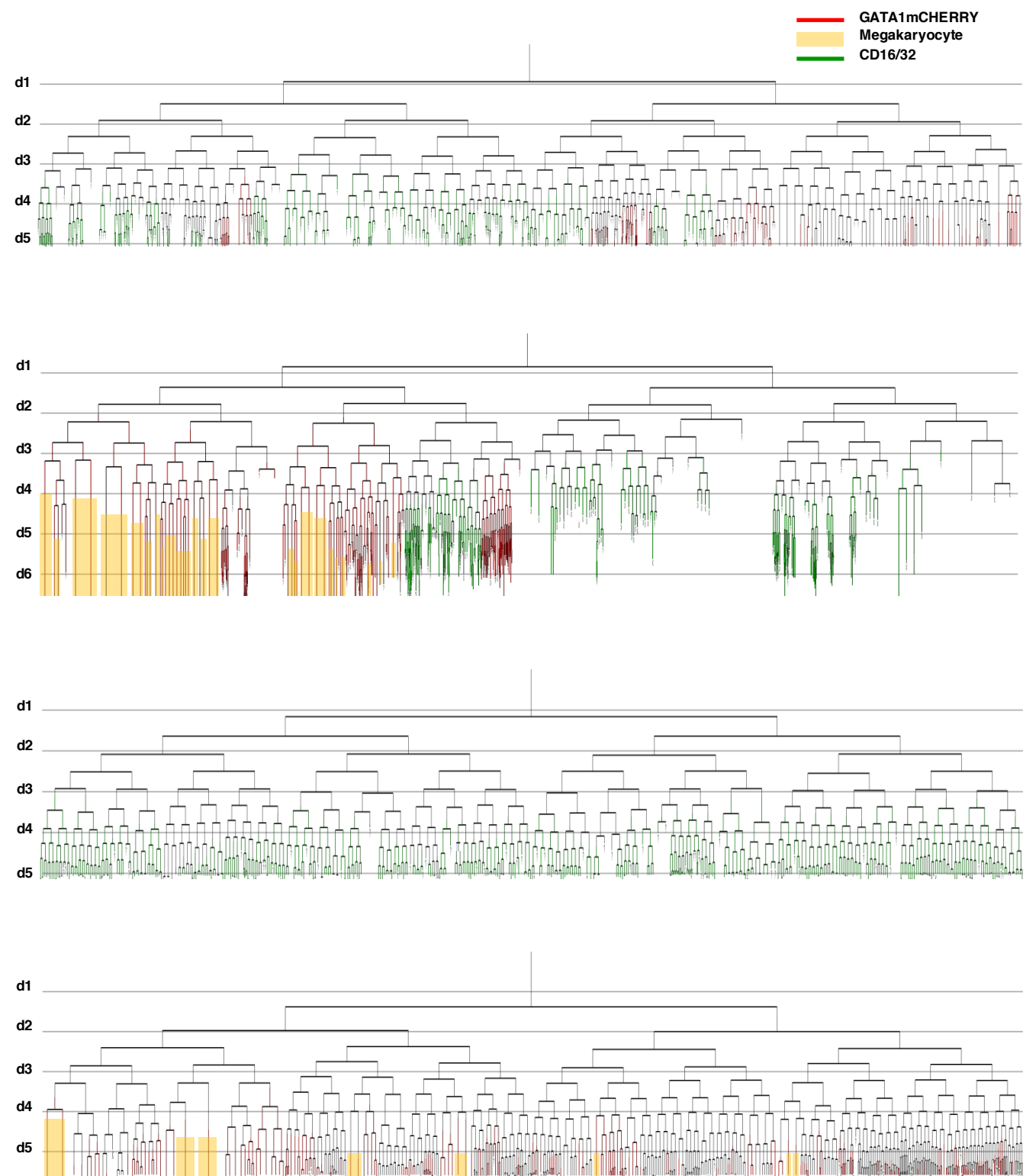


Supplementary Figure 8 | GATA1mCHERRY and PU.1eYFP protein decay is unaltered compared to their wildtype counterparts
a) Western blot quantification of GATA1(mCHERRY) pixel intensities after Cycloheximide treatment of E14.5 fetal liver (FL) cells (50% wildtype C57BL/6, 50% GATA1mCHERRY)
b) Western blot quantification of PU.1(eYFP) pixel intensities after Cycloheximide treatment of PU.1^{wt/eYFP} progenitor cells. No significant differences between paired time-resolved observations between WT and PU.1eYFP or GATA1mCHERRY were detected ($p > 0.16$) (g,h).

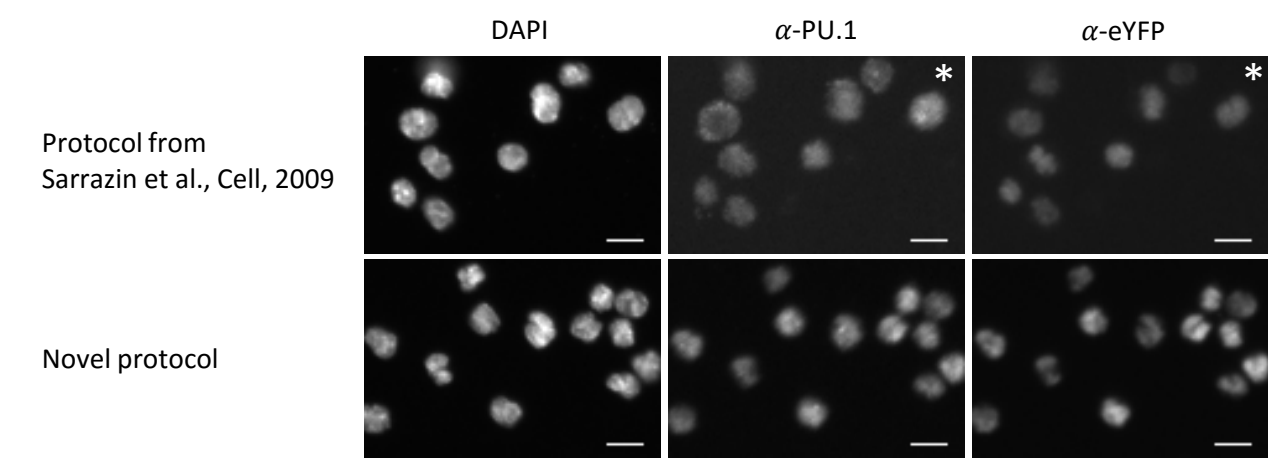


Supplementary Figure 9 | HSCs differentiation kinetics

Single HSCs were sorted into single wells of a 384-well plate. Colonies were observed throughout 10 days by one brightfield image per day. Expression of PU.1eYFP, GATA1mCHERRY and CD16/32 was qualitatively assessed on each day. Colonies were scored into exclusive GATA1mCHERRY+ (white bars), exclusive CD16/32+, or GATA1mCHERRY+ and CD16/32 double-positive (DP) colonies (57%). DP colonies were further discriminated into colonies which started to express GATA1mCHERRY and CD16/32 on the same day (blue bars), expressed GATA1mCHERRY at least one day before CD16/32 (red bars), or expressed CD16/32 before GATA1mCHERRY (green bars). Missing percentages to 100% mean that colonies have either not expressed any marker yet or that individual colonies have died during the course of 10 days. All surviving colonies have turned on at least one marker (GATA1mCHERRY or CD16/32) on day 9. Mean (+ standard deviation) of 3 biological replicates (n=141, 185, 129 colonies).



Supplementary Figure 10 | HSC genealogy examples



Supplementary Figure 11 | Optimized immunostaining protocol enables PU.1 detection

Freshly sorted primary GMPs. Only with the novel protocol, anti-PU.1 staining was located in the nucleus and colocalized with eYFP staining.
Scale bar = 10 μ m.
* Increased contrast to better visualize low signals, all other images within one column were treated the same way.

Supplementary Table 1 | PU.eYFPxGATA1mCHERRY homozygous mice are born at normal mendelian ratios

GATA1 and PU.1	Offspring Frequency Expected		
GATA1 ^{WT} Y PU.1 ^{WT} /WT	3	5,8%	6,3%
GATA1 ^{WT} Y PU.1 ^{WT} /eYFP	5	9,6%	12,5%
GATA1 ^{WT} Y PU.1 ^{eYFP} /eYFP	1	1,9%	6,3%
GATA1 ^{mCHERRY} Y PU.1 ^{WT} /WT	3	5,8%	6,3%
GATA1 ^{mCHERRY} Y PU.1 ^{WT} /eYFP	9	17,3%	12,5%
GATA1 ^{mCHERRY} Y PU.1 ^{eYFP} /eYFP	3	5,8%	6,3%
GATA1 ^{mCHERRY} /WT PU.1 ^{WT} /WT	2	3,8%	6,3%
GATA1 ^{mCHERRY} /WT PU.1 ^{eYFP} /WT	11	21,2%	12,5%
GATA1 ^{mCHERRY} /WT PU.1 ^{eYFP} /eYFP	5	9,6%	6,3%
GATA1 ^{mCHERRY} /mCHERRY PU.1 ^{WT} /WT	2	3,8%	6,3%
GATA1 ^{mCHERRY} /mCHERRY PU.1 ^{eYFP} /WT	5	9,6%	12,5%
GATA1 ^{mCHERRY} /mCHERRY PU.1 ^{eYFP} /eYFP	3	5,8%	6,3%
GATA1			
GATA1 ^{WT} Y	9	17,3%	25,0%
GATA1 ^{mCHERRY} Y	15	28,8%	25,0%
GATA1 ^{mCHERRY} /WT	18	34,6%	25,0%
GATA1 ^{mCHERRY} /mCHERRY	10	19,2%	25,0%
PU.1			
PU.1 ^{WT} /WT	10	19,2%	25,0%
PU.1 ^{eYFP} /WT	30	57,7%	50,0%
PU.1 ^{eYFP} /eYFP	12	23,1%	25,0%

Offspring of the mating ♂ GATA1^{mCHERRY}Y PU.1^{eYFP}/WT x ♀ GATA1^{mCHERRY}/WT PU.1^{eYFP}/WT
Shown are real and expected frequencies for the respective genotypes.

Supplementary Table 2 | Protein abundance in different cell populations in FACS and imaging

FACS		
Cell population	PU.1eYFP	GATA1mCHERRY
PU.1 ⁺ GATA1 ⁻ LK progenitor	43.1 ± 10.6 · 10 ³	NA
E14.5 GATA1 ⁺ fetal liver	NA	23.0 ± 9.8 · 10 ³
PU.1 ^{high} GATA1 ⁻	47.3 ± 12.9 · 10 ³	-- / Below negative gate
PU.1 ^{mid} GATA1 ^{mid}	5.9 ± 1.8 · 10 ³	25.5 ± 12.3 · 10 ³
PU.1-GATA1 ^{high}	-- / Below negative gate	54.6 ± 23.8 · 10 ³
HSC	8.1 ± 2.1 · 10 ³	-- / Below negative gate
LSK	16.4 ± 4.3 · 10 ³	-- / Below negative gate
GMP	42.7 ± 11.7 · 10 ³	-- / Below negative gate
MEP	-- / Below negative gate	49.4 ± 21.4 · 10 ³
Negative gate (GMP)	4.4 ± 1.2 · 10 ³	6.5 ± 3.8 · 10 ³
Negative gate (MEP)	4.7 ± 1.5 · 10 ³	8.4 ± 4.6 · 10 ³

Imaging		
Cell population	PU.1eYFP	GATA1mCHERRY
PU.1 ^{high} GATA1 ⁻	47.3 ± 12.9 · 10 ³	-- / Below negative gate
PU.1 ^{mid} GATA1 ^{mid}	5.5 ± 4.4 · 10 ³	25.6 ± 16.3 · 10 ³
PU.1-GATA1 ^{high}	-- / Below negative gate	54.6 ± 23.8 · 10 ³
HSC	8.1 ± 2.1 · 10 ³	-- / Below negative gate
GMP	40.1 ± 4.7 · 10 ³	-- / Below negative gate
Negative gate (in silico)	1.1 ± 2.0 · 10 ³	1.9 ± 4.4 · 10 ³

Calculated PU.1eYFP and GATA1mCHERRY protein molecule numbers both for FACS and imaging for the respective cell populations as well as the negative gates, i.e. the detection thresholds.

Supplementary Table 3 | Data overview from time-lapse movies

	Movie 1	Movie 2	Movie 3	Movie 4	All Movies
Starting cells	63	61	62	70	256
Early Apoptosis (<48h)	15	16	8	7	46
Early Apoptosis (<48h) %	23,8%	26,2%	12,9%	10,0%	18,2%
Lost without onset	5	1	0	3	9
Lost without onset %	7,9%	1,6%	0,0%	4,3%	3,5%
Trees with onsets	34	32	31	51	148
Trees with onsets %	54,0%	52,5%	50,0%	72,9%	57,4%
Trees without onsets	9	12	23	9	53
Trees without onsets %	14,3%	19,7%	37,1%	12,9%	21,0%
GM onsets	227	146	163	544	1080
ME onsets	89	230	93	269	681
Starting cells with >0 GM onset	31	20	19	31	101
Starting cells with >0 ME onset	8	16	17	29	70
Double positive trees	6	4	5	8	23
Trees with >1 GM (and no ME) onset	25	16	14	23	78
Trees with >1 ME (and no GM) onset	2	12	12	21	47
Deepest tracked division per tree (Mean)	6,6	6,0	7,0	7,8	6,9
Standard Deviation	4,5	4,4	3,2	3,7	4,0
Trees with max. 0 divisions	12	11	3	4	30
Trees with max. 1 divisions	2	3	1	3	9
Trees with max. 2 divisions	0	1	3	1	5
Trees with max. 3 divisions	0	0	1	2	3
Trees with max. 4 divisions	1	2	4	0	7
Trees with max. 5 divisions	1	1	4	4	10
Trees with max. 6 divisions	1	0	6	6	13
Trees with max. 7 divisions	2	2	4	4	12
Trees with max. 8 divisions	6	3	4	3	16
Trees with max. 9 divisions	8	8	12	6	34
Trees with max. 10 divisions	5	9	7	14	35
Trees with max. 11 divisions	6	2	3	5	16
Trees with max. 12 divisions	3	2	2	7	14
Trees with max. 13 divisions	1	0	0	1	2
Mean Onset per Tree (if >0 onsets)	6,0	4,1	5,1	5,4	5,2
Mean Standard Deviation	2,6	3,5	2,8	3,1	3,0
Mean Onset Generation 0	4	10	4	10	28
Mean Onset Generation 1	0	3	2	0	5
Mean Onset Generation 2	0	1	1	0	2
Mean Onset Generation 3	1	0	1	1	3
Mean Onset Generation 4	0	2	2	2	6
Mean Onset Generation 5	4	1	4	7	16
Mean Onset Generation 6	9	2	4	8	23
Mean Onset Generation 7	7	6	7	8	28
Mean Onset Generation 8	5	5	5	9	24
Mean Onset Generation 9	3	2	1	4	10
Mean Onset Generation 10	1	0	0	1	2
Mean Onset Generation 11	0	0	0	0	0
Mean Onset Generation 12	0	0	0	0	0
Mean Onset Generation 13	0	0	0	0	0

Overview about how many colonies per independent movie were tracked and their respective fate outcome, the amount of colonies regarding their latest tracked division and the amount of colonies regarding their mean marker onset (GATA1mCHERRY and/or CD16/32). General tree fates include “apoptosis” (<48h after moviestart), “lost” (no information because cells moved out of the eyefield or got mixed up with other cells), “onset” (at least one marker onset per tracked tree) and “no onset” (no marker onset in tracked tree).

Supplementary Movie 1 | HSC progeny differentiating into GM cells does not express GATA1

Cell genealogy starting from an HSC, displaying one consecutive daughter cell each in brightfield images (,BF‘) with PU.1eYFP signal (,PU.1‘), GATA1mCHERRY signal (,Gata1‘) and CD16/32 expression (, CD16/32‘) determined by live antibody staining. Time format (relative to movie start): d (day) – hh (hours):mm (minutes):ss (seconds).

Supplementary Movie 2 | HSC progeny differentiating into MegE cells downregulate PU.1 before GATA1 is expressed

Cell genealogy starting from an HSC, displaying one consecutive daughter cell each in brightfield images (,BF‘) with PU.1eYFP signal (,PU.1‘), GATA1mCHERRY signal (,Gata1‘) and CD16/32 expression (, CD16/32‘) determined by live antibody staining. Time format (relative to movie start): d (day) – hh (hours):mm (minutes):ss (seconds).

Supplementary Movie 3 | PU.1 and GATA1 protein expression during early myeloid lineage choice

Density scatter plot of PU.1eYFP and GATA1mCHERRY expression levels during differentiation of all tracked HSCs with CD16/32 or GATA1mCHERRY expression (see also Fig. 4h). Normalized to the onset (t=0h) of CD16/32 and GATA1mCHERRY, respectively. Light blue circle highlights initial expression profile of HSCs.